

Supporting Information for:

Selective and Sensitive Sensing of Hydrogen Peroxide by a Boronic Acid Functionalized Metal-Organic Framework and its Application in Live-Cell Imaging

Mostakim SK,[†] Sooram Banesh,[‡] Vishal Trivedi,[‡] and Shyam Biswas^{*,†}

[†] Department of Chemistry, Indian Institute of Technology Guwahati, Guwahati, 781039 Assam, India

[‡] Malaria Research Group, Department of Biosciences and Bioengineering, Indian Institute of Technology Guwahati, 781039 Assam, India

*To whom correspondence should be addressed. E-mail: sbiswas@iitg.ernet.in; Tel: 91-3612583309

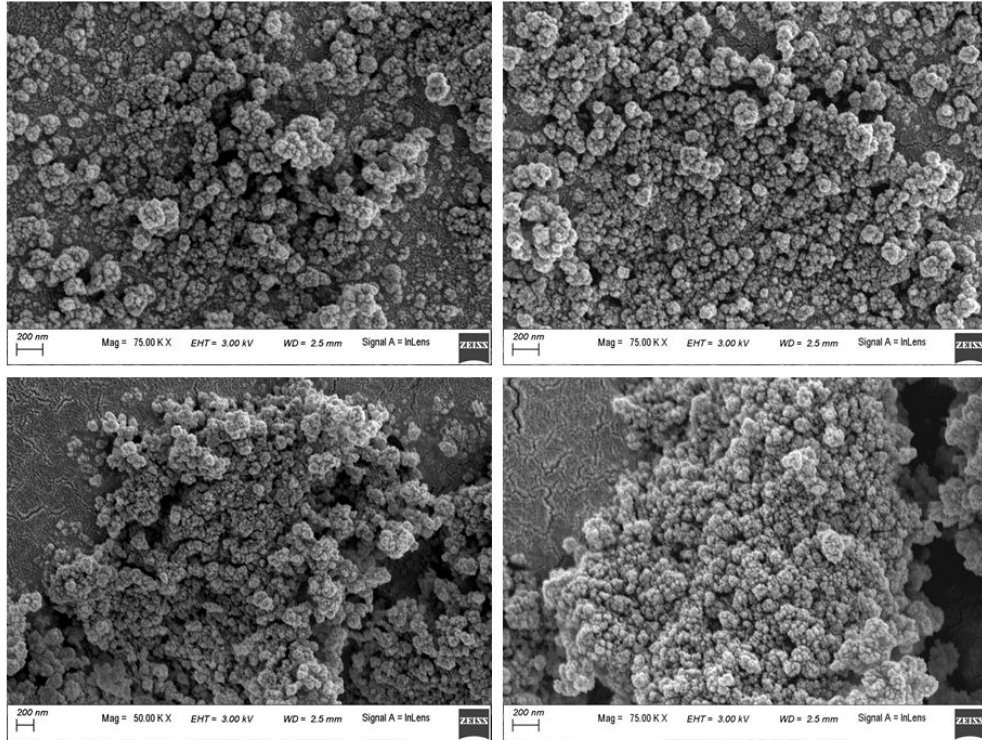


Figure S1. FE-SEM images of 1.

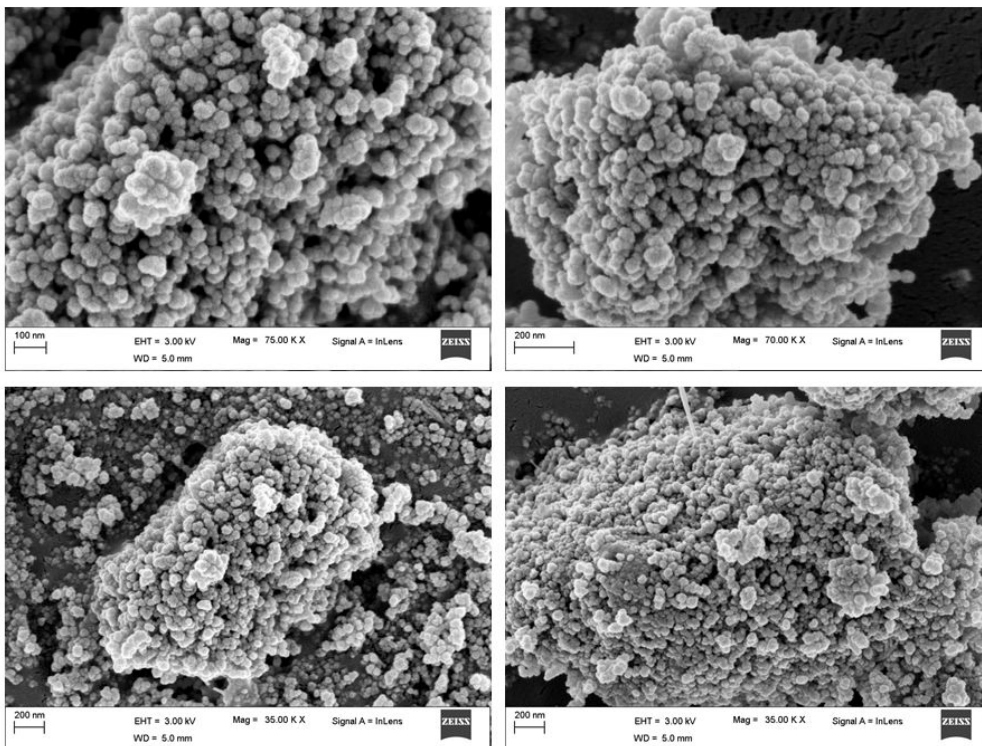


Figure S2. FE-SEM images of 1'.

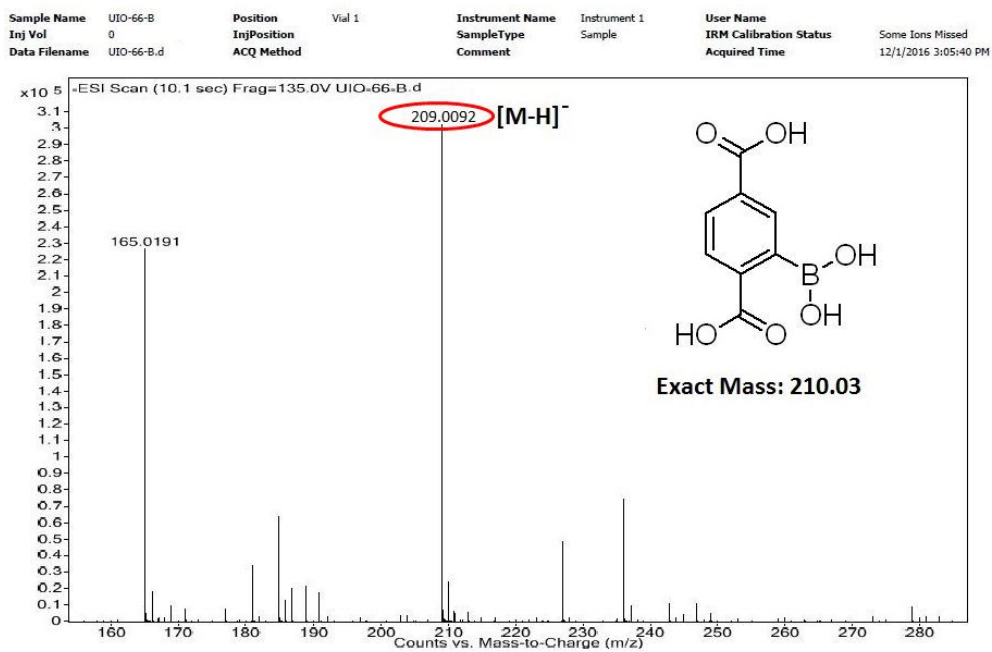


Figure S3. ESI-MS spectrum of 1' after digestion in methanol/HF.

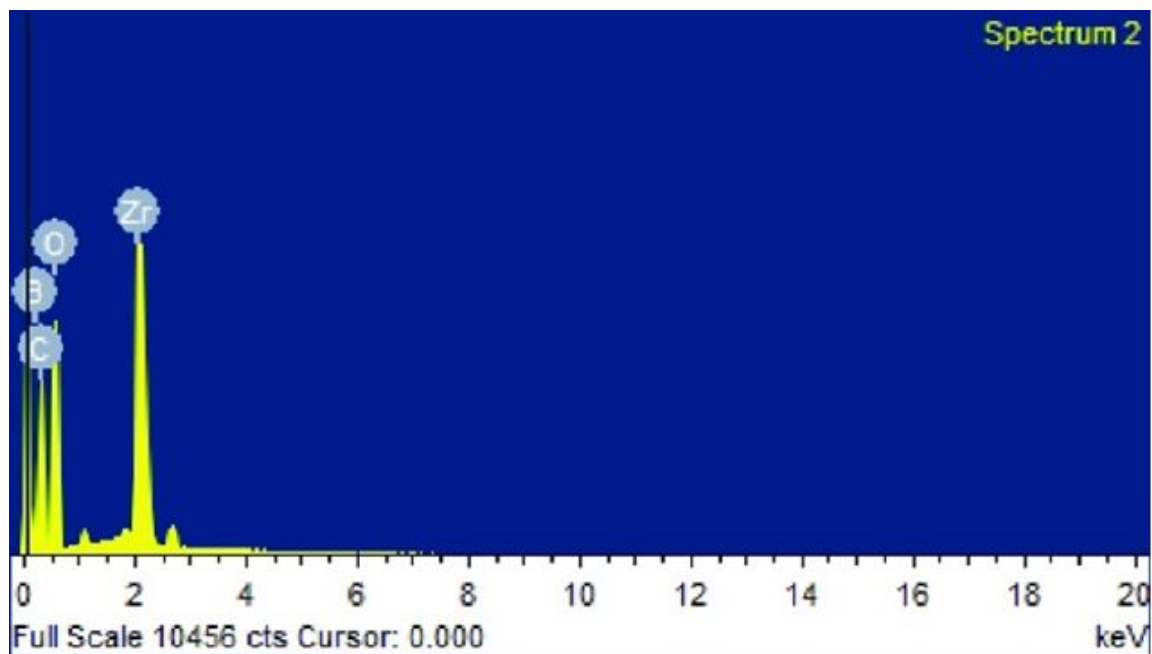


Figure S4. EDX spectrum of 1'.

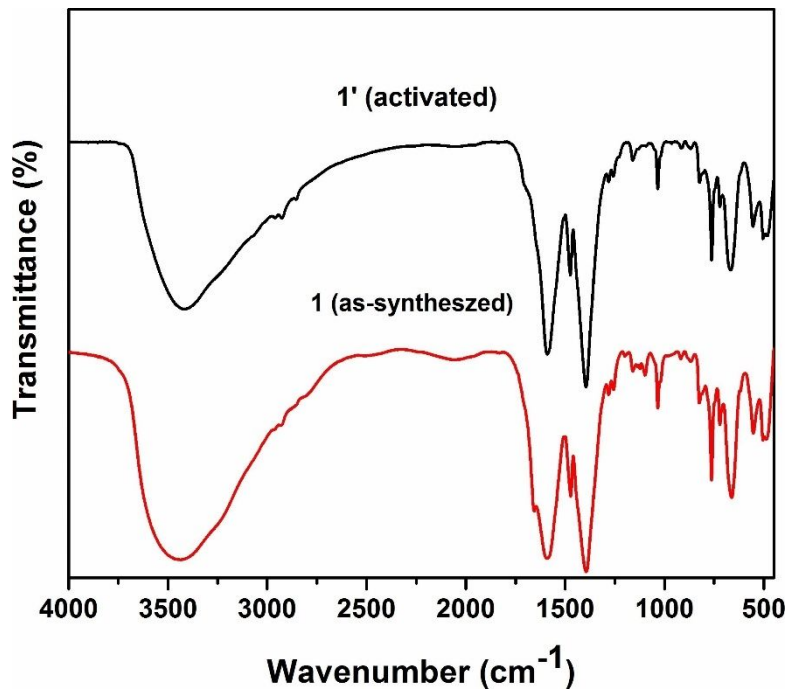


Figure S5. FT-IR spectra of as-synthesized 1 (red) and activated 1' (black).

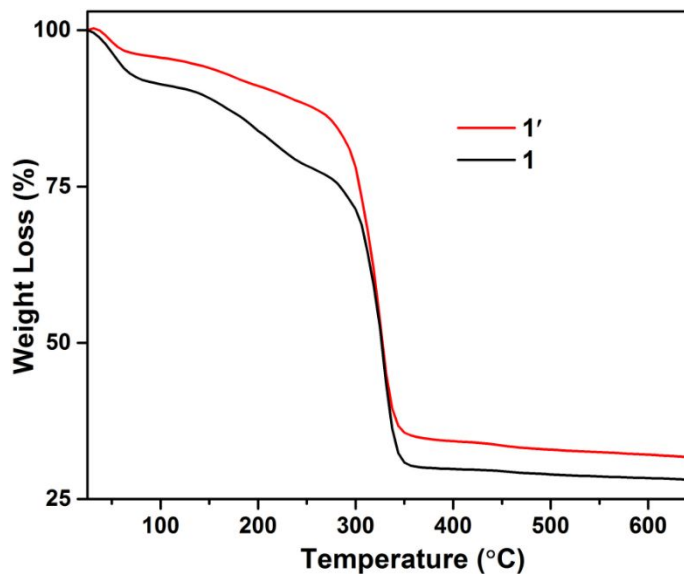


Figure S6. TG curve of as-synthesized (red) and activated (black) of **1'** measured under air atmosphere with a heating rate of 5 °C min⁻¹.

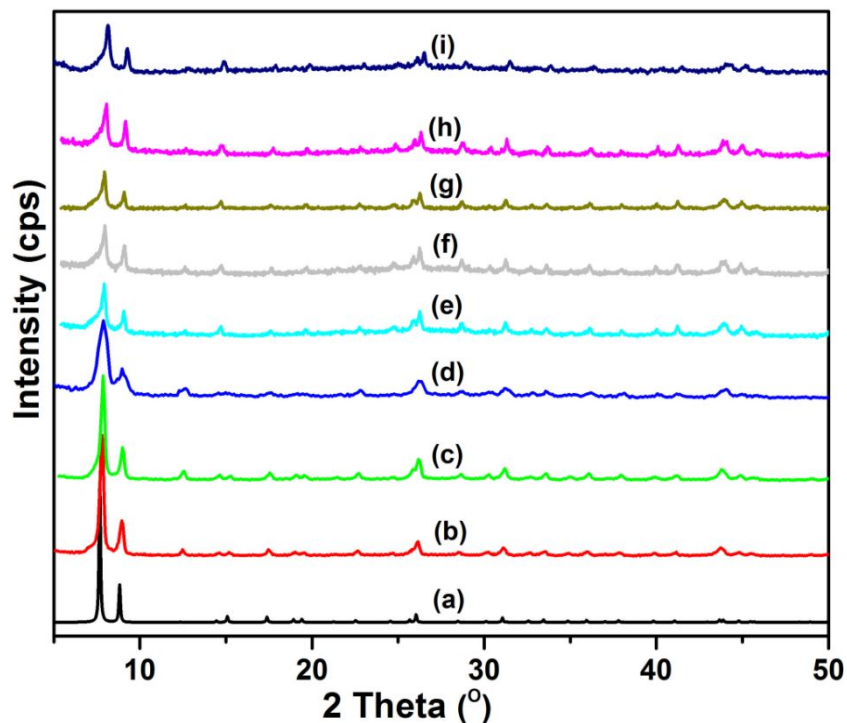


Figure S7. XRPD patterns of **1'** in different forms: calculated (a); as-synthesized (b); activated (c); after BET measurement (d); after treatment with water (e); after H₂O₂ sensing experiment (in 10 mM HEPES buffer at pH = 7.4) (f); after treatment with 1(M) HCl (g); after treatment with acetic acid (h); after treatment with NaOH at pH = 10 (i).

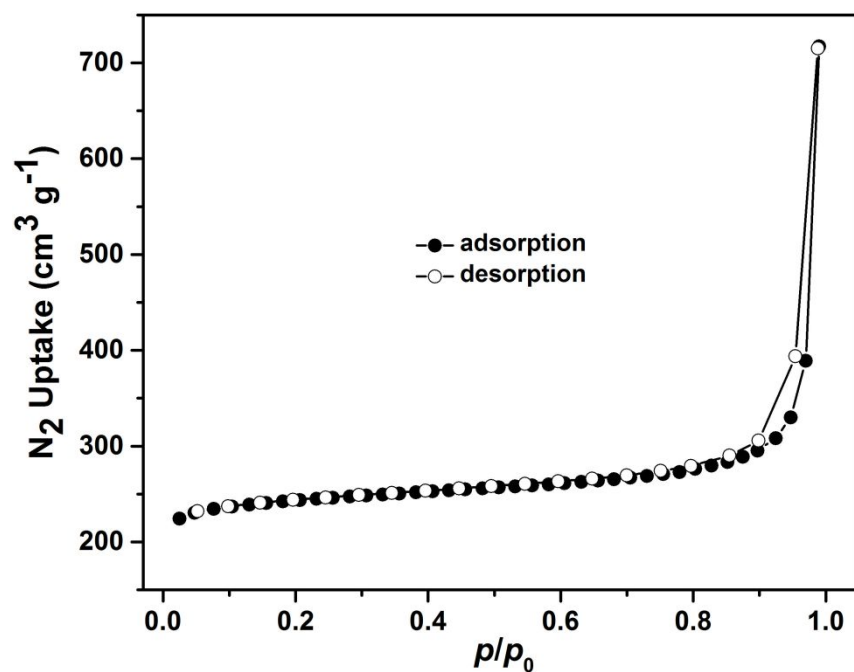


Figure S8. N₂ adsorption (filled circles) and desorption (empty circles) isotherms of **1'** measured at -196 °C.

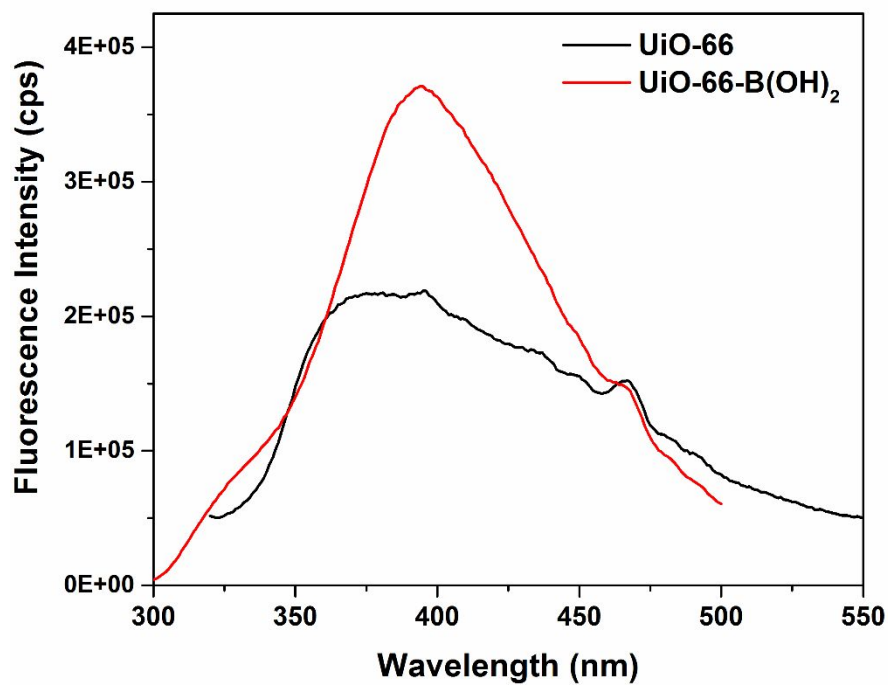


Figure S9. Fluorescence emission spectra of UiO-66 and UiO-66-B(OH)₂ compounds.

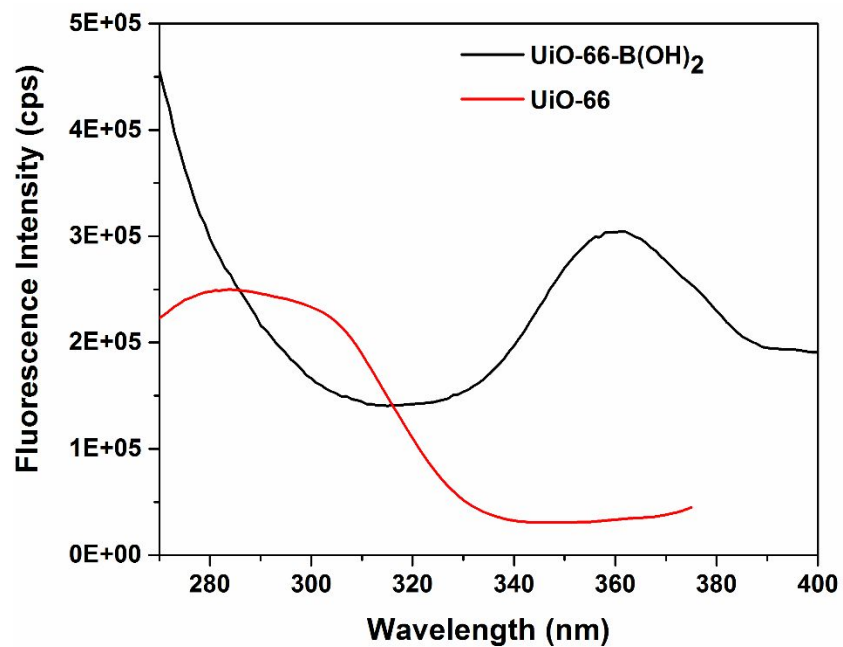


Figure S10. Fluorescence excitation spectra of UiO-66 and UiO-66-B(OH)₂ compounds.

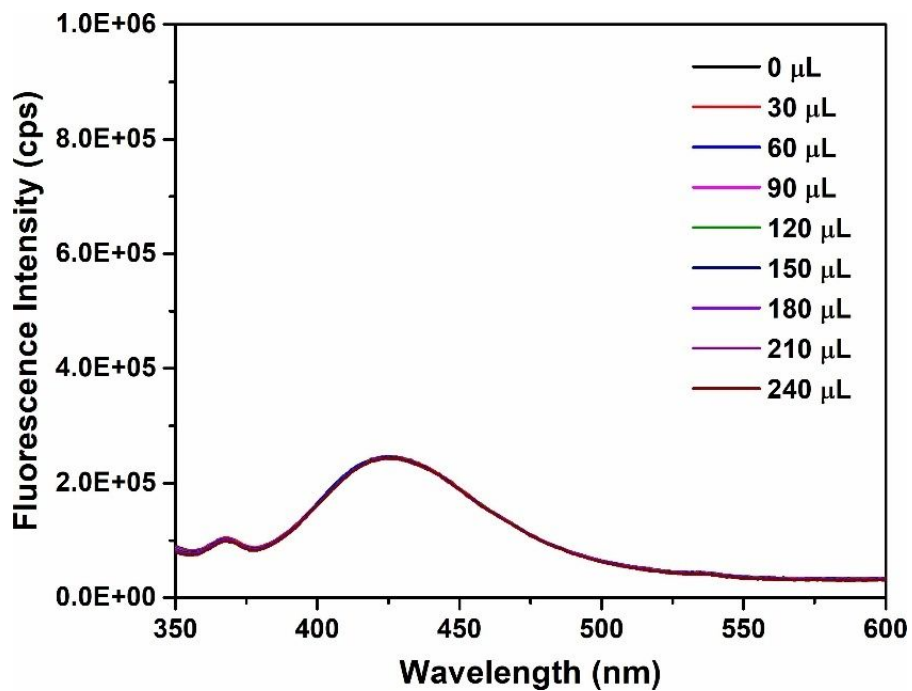


Figure S11. Fluorescence response of **1'** towards 10 mM NaOCl ($\lambda_{\text{ex}} = 328$ nm and $\lambda_{\text{em}} = 426$ nm).

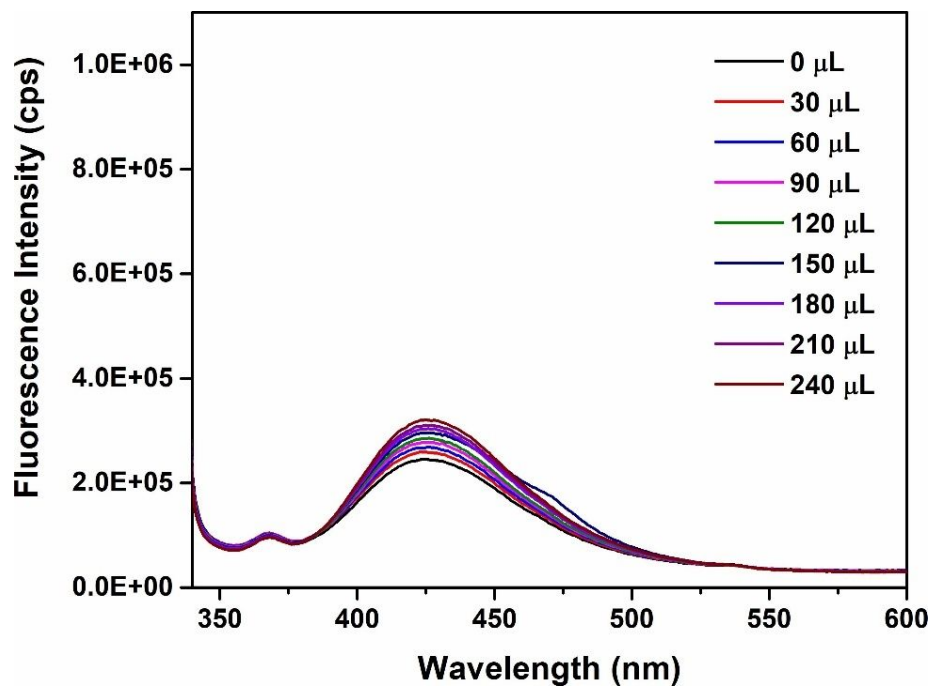


Figure S12. Fluorescence response of **1'** towards 10 mM $O_2^{\bullet-}$ ($\lambda_{\text{ex}} = 328$ nm and $\lambda_{\text{em}} = 426$ nm).

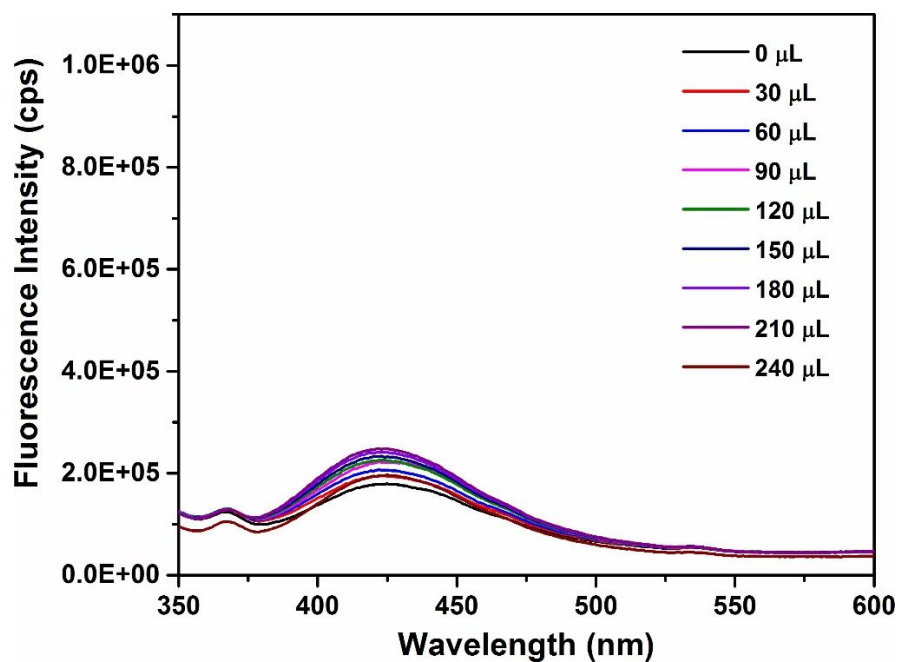


Figure S13. Fluorescence response of **1'** towards 10 mM $t\text{BuO}^{\bullet}$ ($\lambda_{\text{ex}} = 328$ nm and $\lambda_{\text{em}} = 426$ nm).

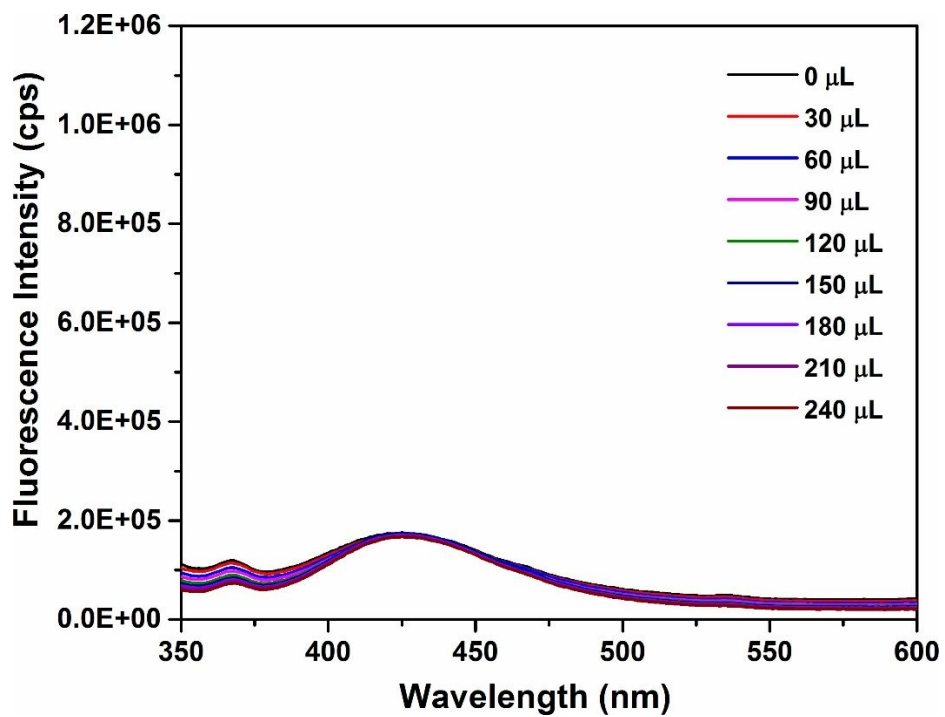


Figure S14. Fluorescence response of **1'** towards 10 mM HO• ($\lambda_{\text{ex}} = 328$ nm and $\lambda_{\text{em}} = 426$ nm).

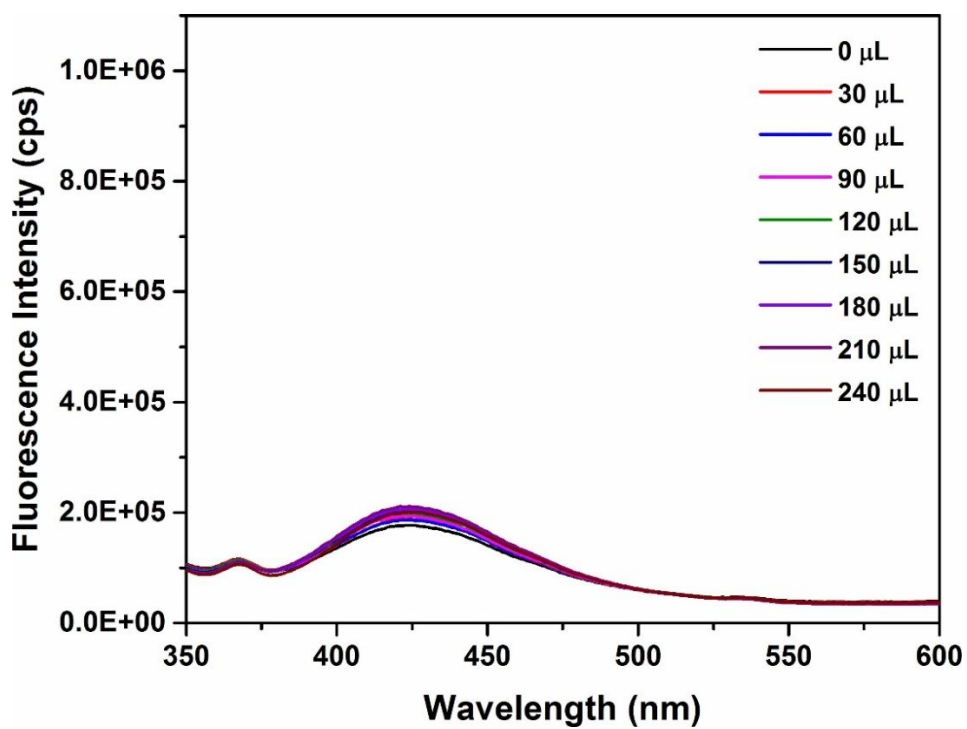


Figure S15. Fluorescence response of **1'** towards 10 mM TBHP ($\lambda_{\text{ex}} = 328$ nm and $\lambda_{\text{em}} = 426$ nm).

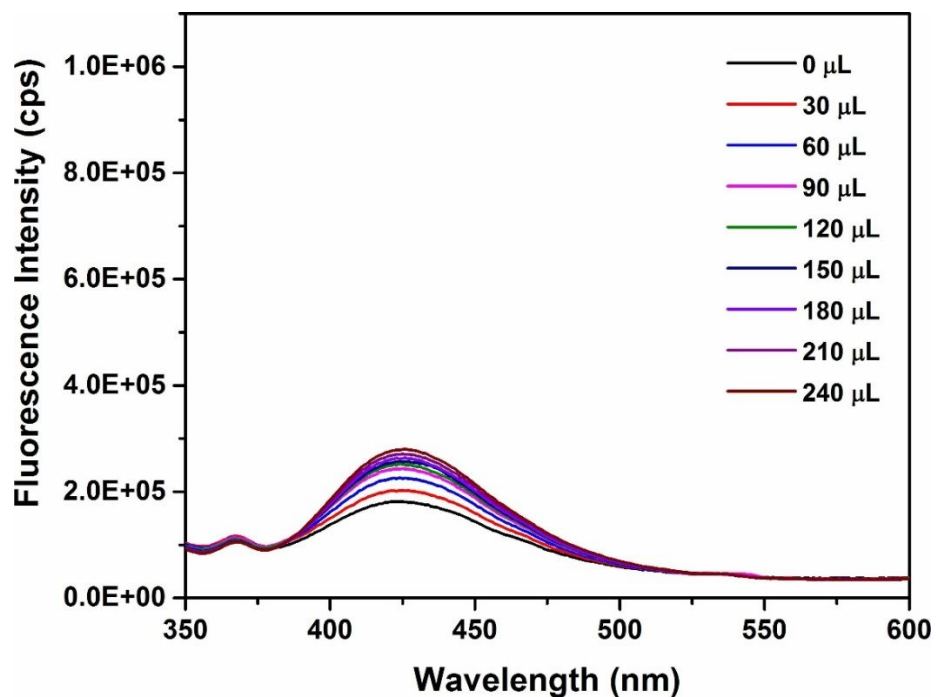


Figure S16. Fluorescence response of **1'** towards 10 mM $^1\text{O}_2$ ($\lambda_{\text{ex}} = 328$ nm and $\lambda_{\text{em}} = 426$ nm).

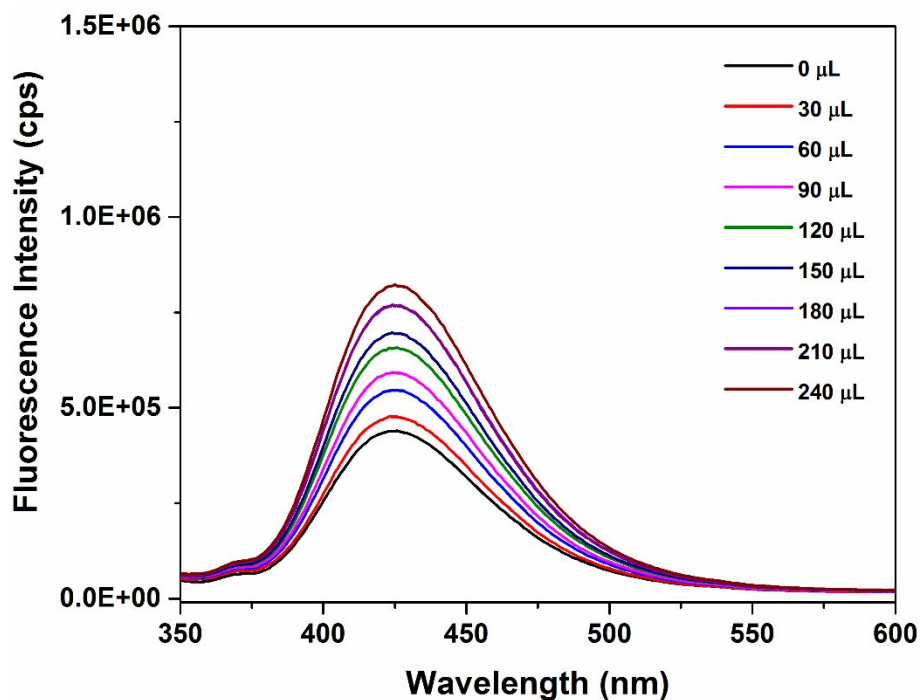


Figure S17. Fluorescence response of **1'** towards 10 mM F^- ion ($\lambda_{\text{ex}} = 328$ nm and $\lambda_{\text{em}} = 426$ nm).

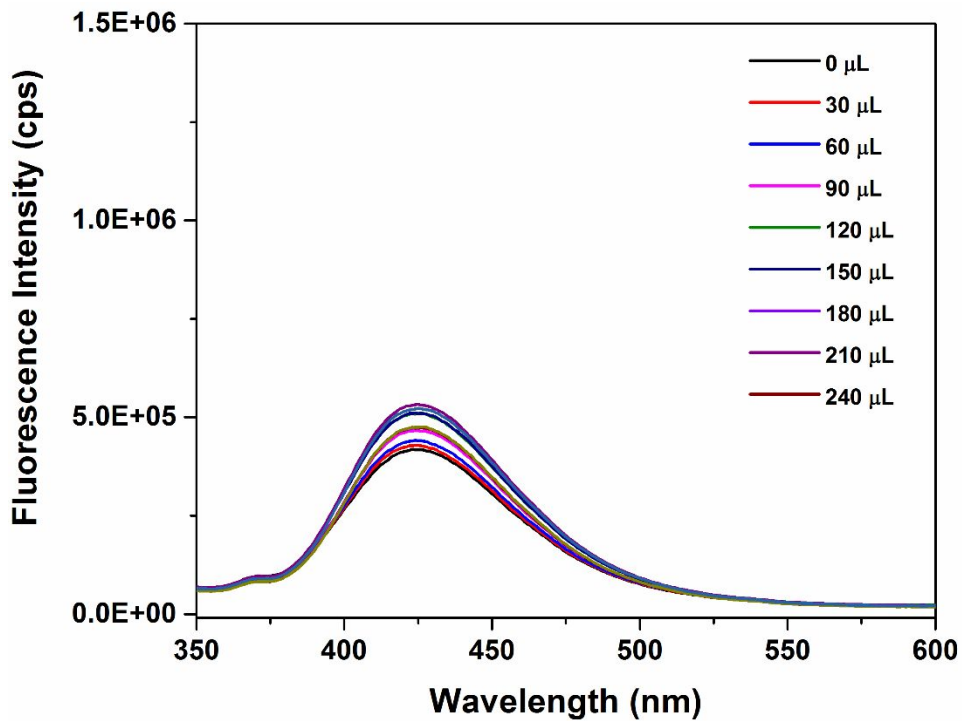


Figure S18. Fluorescence response of **1'** towards 10 mM glucose ($\lambda_{\text{ex}} = 328$ nm and $\lambda_{\text{em}} = 426$ nm).

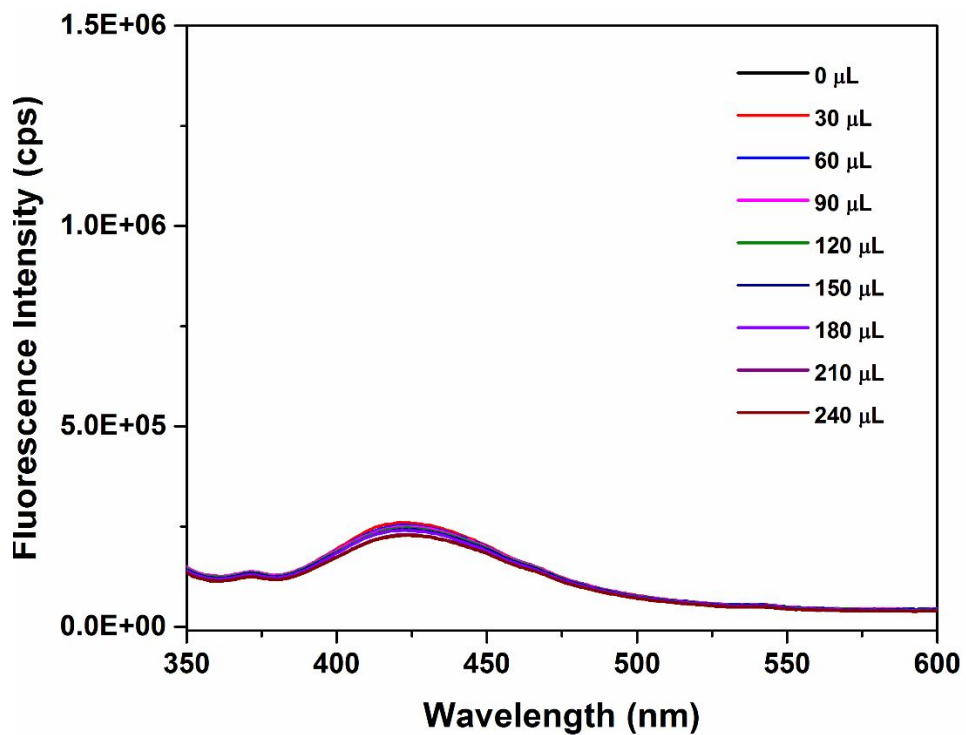


Figure S19. Fluorescence response of **1'** towards 10 mM fructose ($\lambda_{\text{ex}} = 328$ nm and $\lambda_{\text{em}} = 426$ nm).

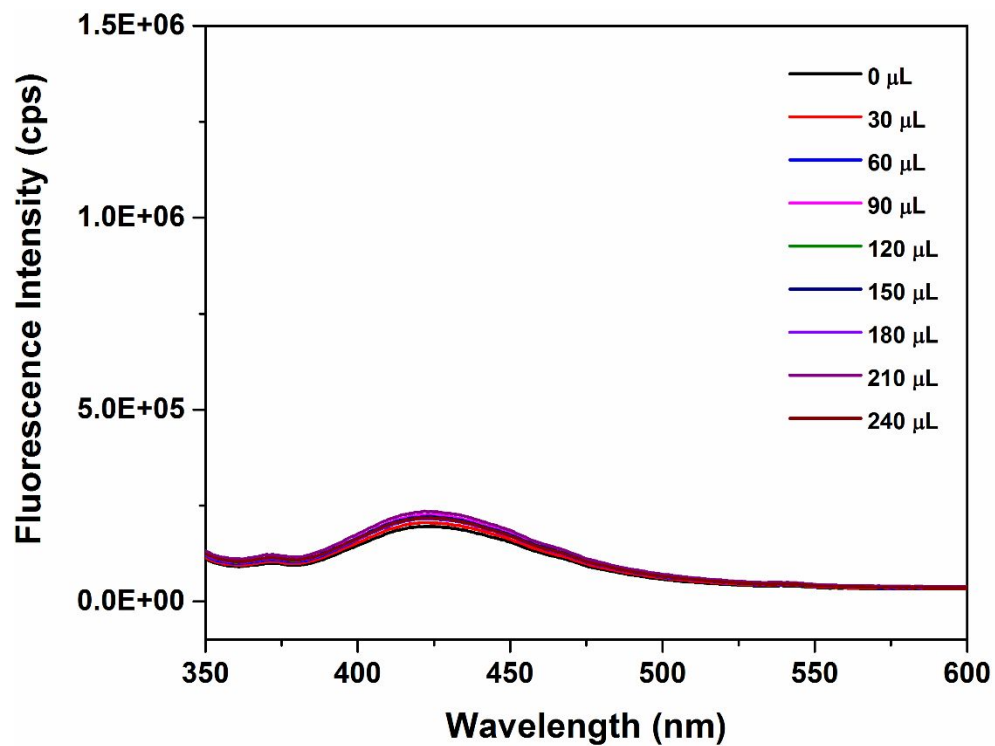


Figure S20. Fluorescence response of **1'** towards 10 mM galactose ($\lambda_{\text{ex}} = 328$ nm and $\lambda_{\text{em}} = 426$ nm).

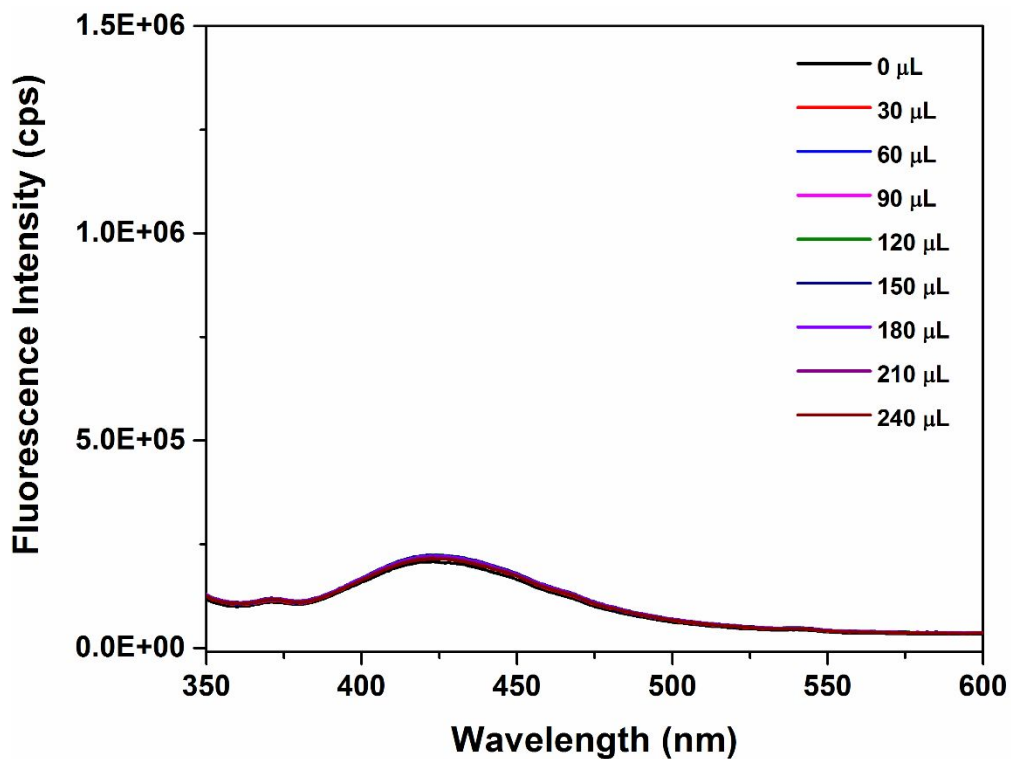


Figure S21. Fluorescence response of **1'** towards 10 mM mannose ($\lambda_{\text{ex}} = 328$ nm and $\lambda_{\text{em}} = 426$ nm).

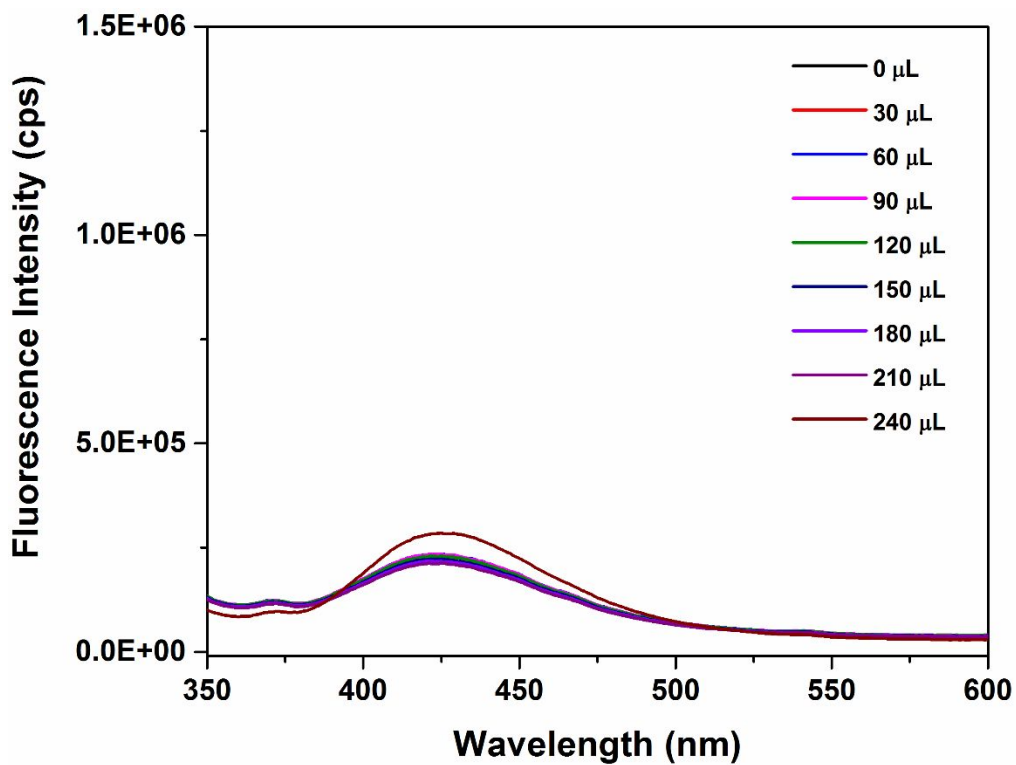


Figure S22. Fluorescence response of **1'** towards 10 mM xylose ($\lambda_{\text{ex}} = 328 \text{ nm}$ and $\lambda_{\text{em}} = 426 \text{ nm}$).

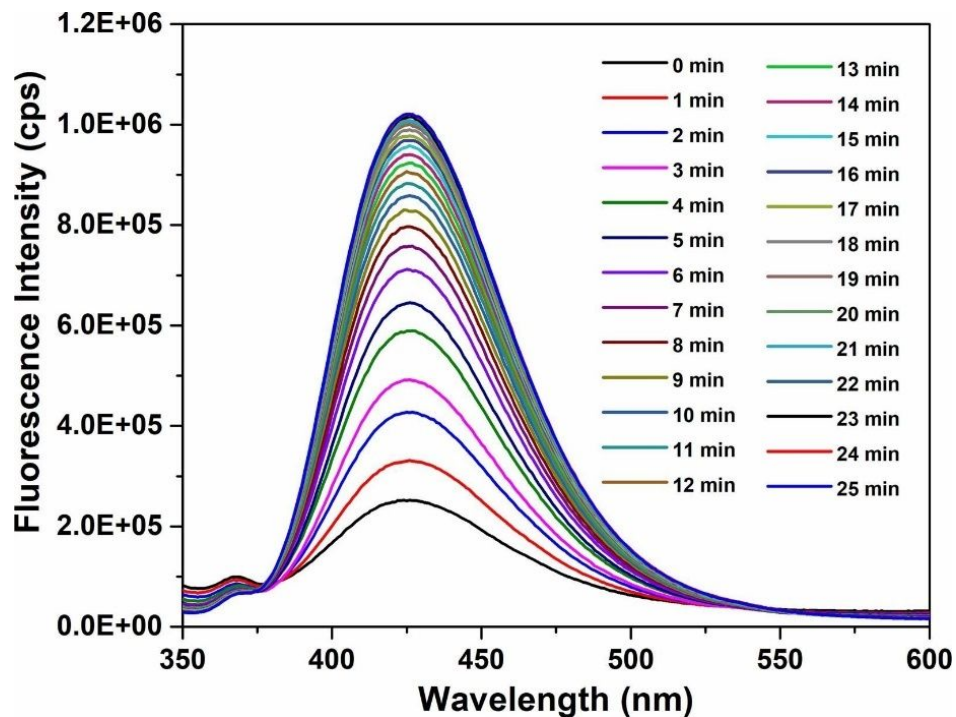


Figure S23. Change in the fluorescence spectrum of **1'** in presence of 10 mM H_2O_2 as a function of time ($\lambda_{\text{ex}} = 328 \text{ nm}$ and $\lambda_{\text{em}} = 426 \text{ nm}$).

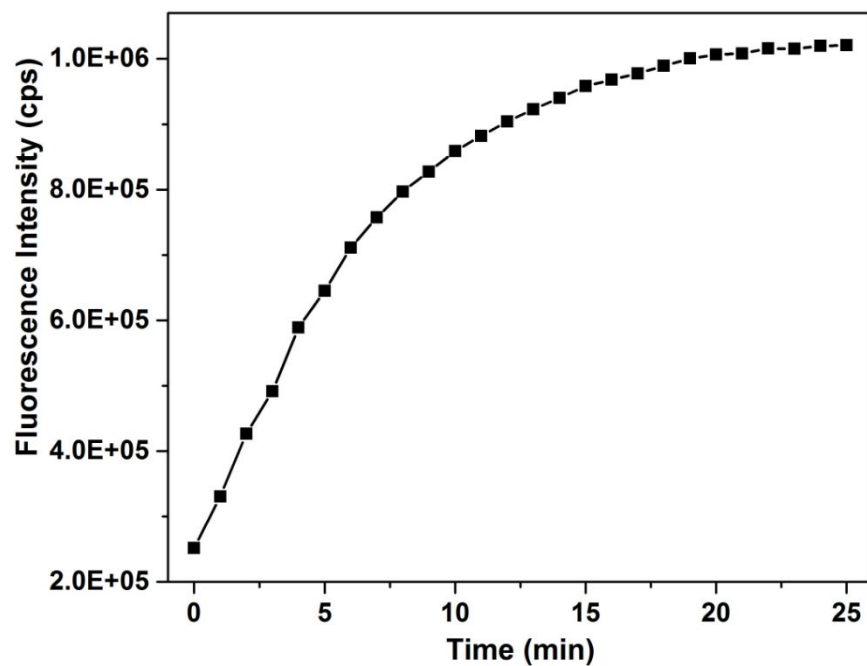


Figure S24. Change in the fluorescence intensity of **1'** in presence of 10 mM H₂O₂ as a function of time ($\lambda_{\text{ex}} = 328$ nm and $\lambda_{\text{em}} = 426$ nm).

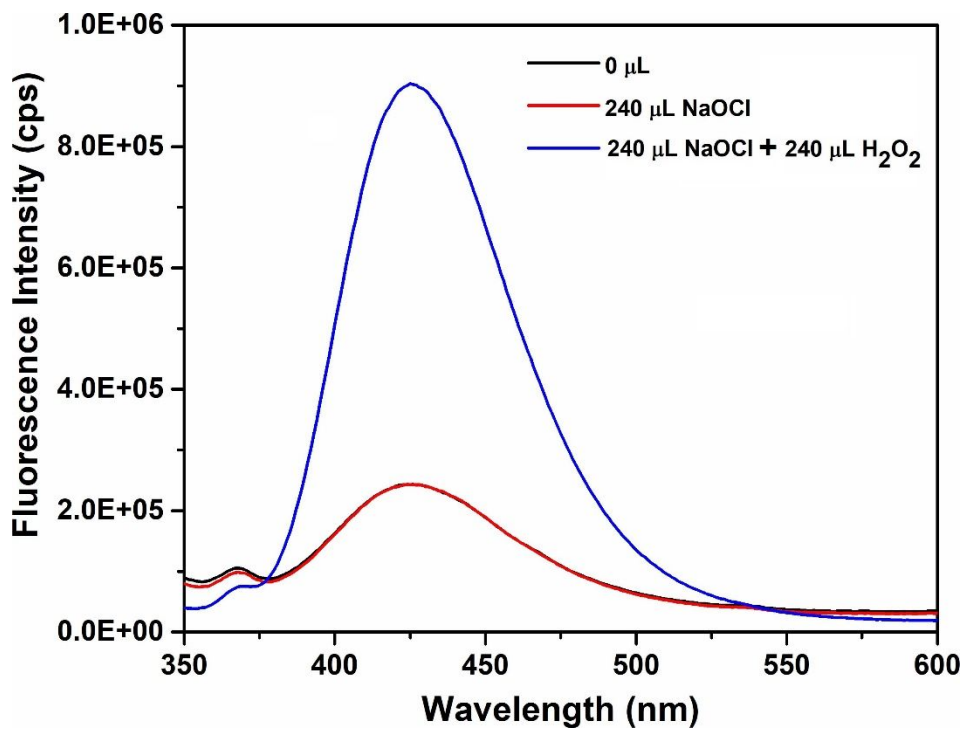


Figure S25. Fluorescence response of **1'** towards 10 mM H₂O₂ in presence of 10 mM NaOCl ($\lambda_{\text{ex}} = 328$ nm and $\lambda_{\text{em}} = 426$ nm).

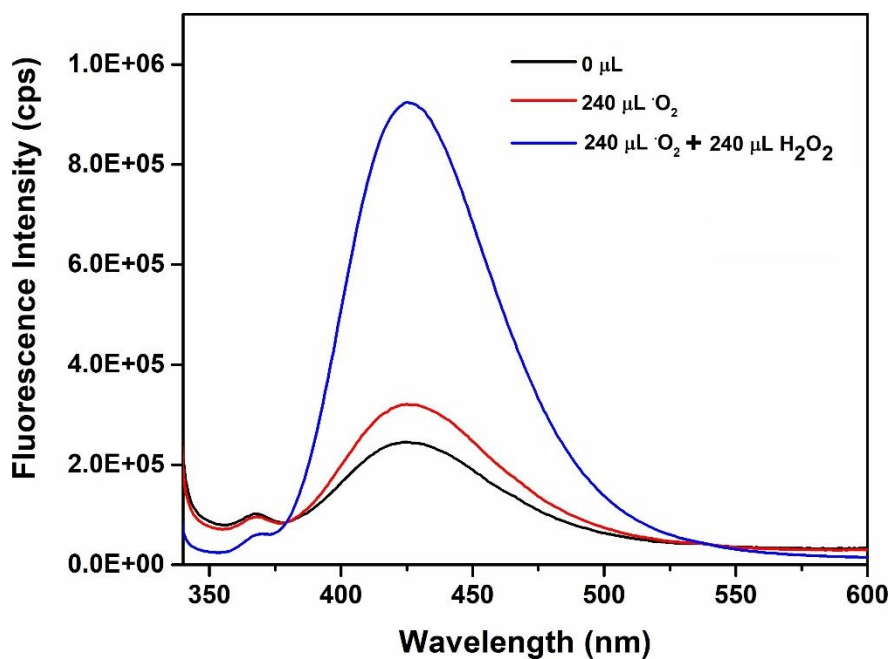


Figure S26. Fluorescence response of **1'** towards 10 mM H₂O₂ in presence of 10 mM O₂⁻ ($\lambda_{\text{ex}} = 328$ nm and $\lambda_{\text{em}} = 426$ nm).

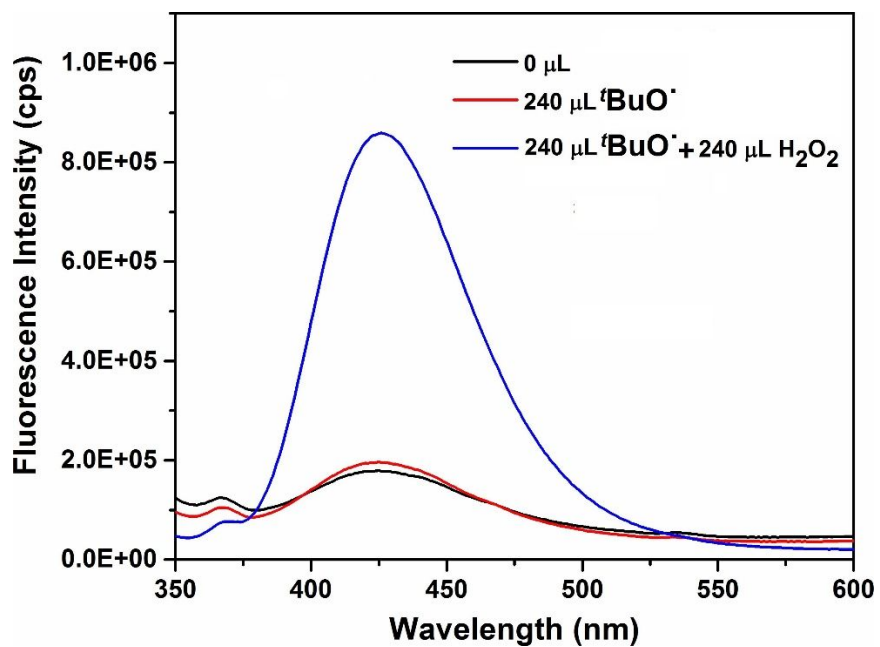


Figure S27. Fluorescence response of **1'** towards 10 mM H₂O₂ in presence of 10 mM tBuO· ($\lambda_{\text{ex}} = 328$ nm and $\lambda_{\text{em}} = 426$ nm).

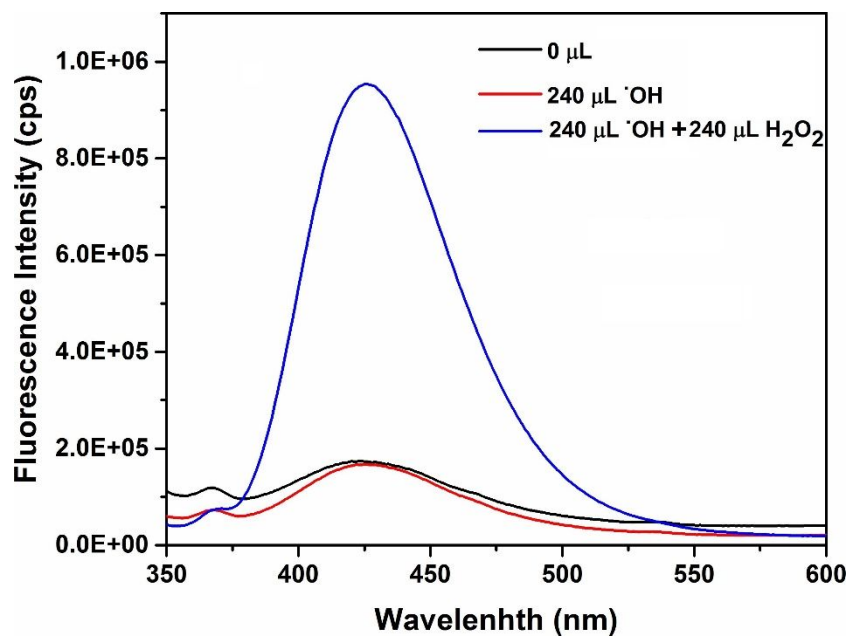


Figure S28. Fluorescence response of **1'** towards 10 mM H₂O₂ in presence of 10 mM HO• ($\lambda_{\text{ex}} = 328$ nm and $\lambda_{\text{em}} = 426$ nm).

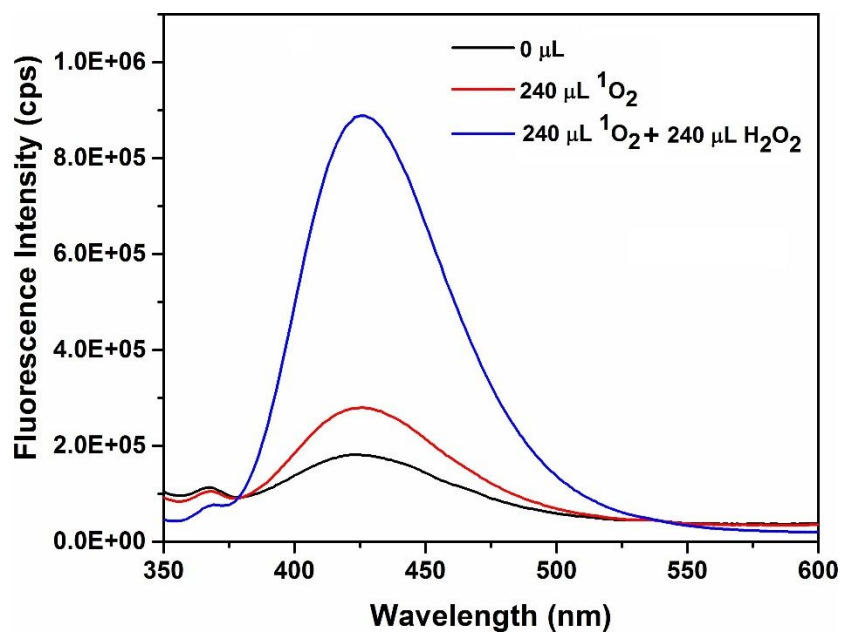


Figure S29. Fluorescence response of **1'** towards 10 mM H₂O₂ in presence of 10 mM ¹O₂ ($\lambda_{\text{ex}} = 328$ nm and $\lambda_{\text{em}} = 426$ nm).

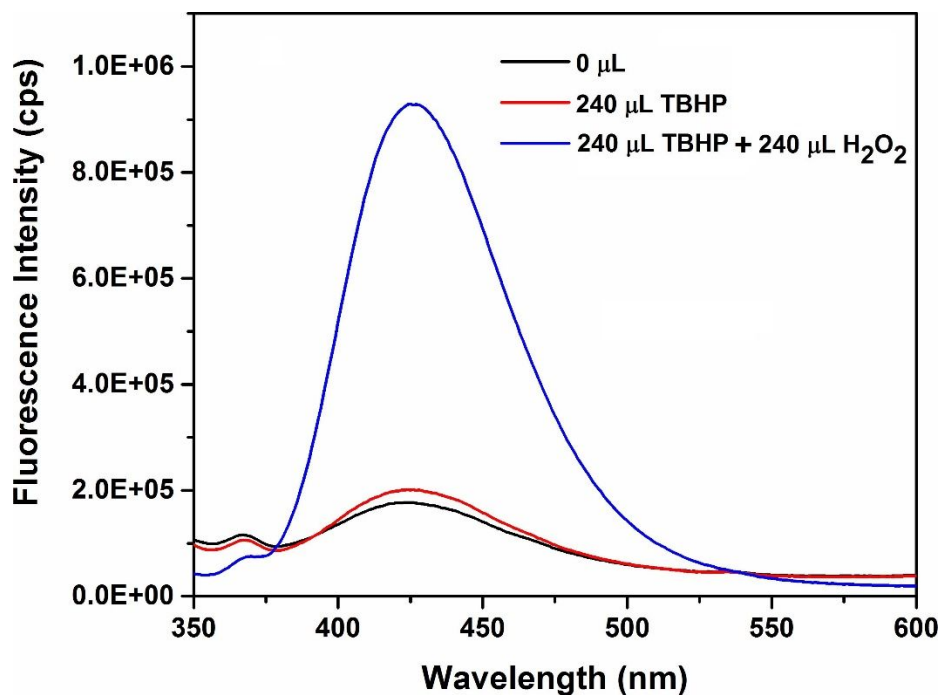


Figure S30. Fluorescence response of **1'** towards 10 mM H₂O₂ in presence of 10 mM TBHP (λ_{ex} = 328 nm and λ_{em} = 426 nm).

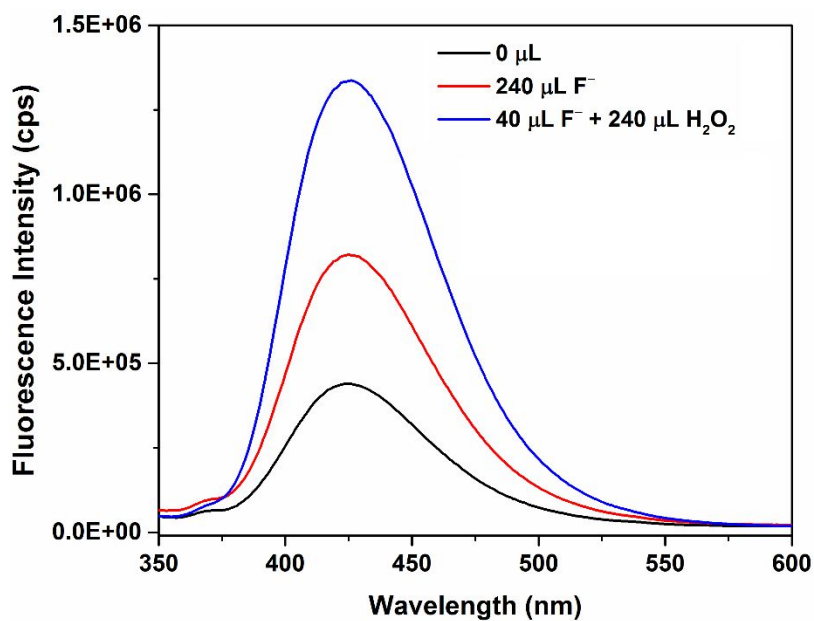


Figure S31. Fluorescence response of **1'** towards 10 mM H₂O₂ in presence of 10 mM F⁻ (λ_{ex} = 328 nm and λ_{em} = 426 nm).

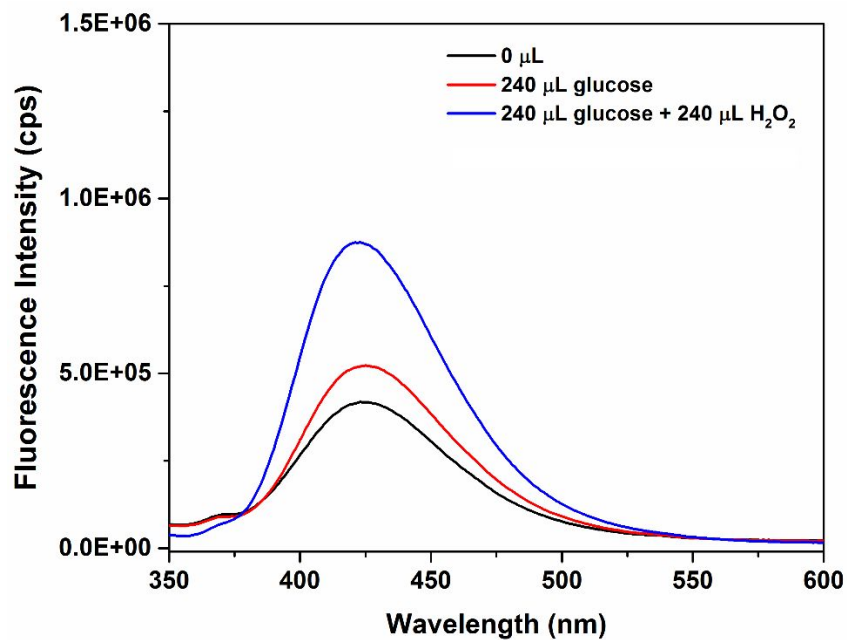


Figure S32. Fluorescence response of **1'** towards 10 mM H_2O_2 in presence of 10 mM glucose ($\lambda_{\text{ex}} = 328$ nm and $\lambda_{\text{em}} = 426$ nm).

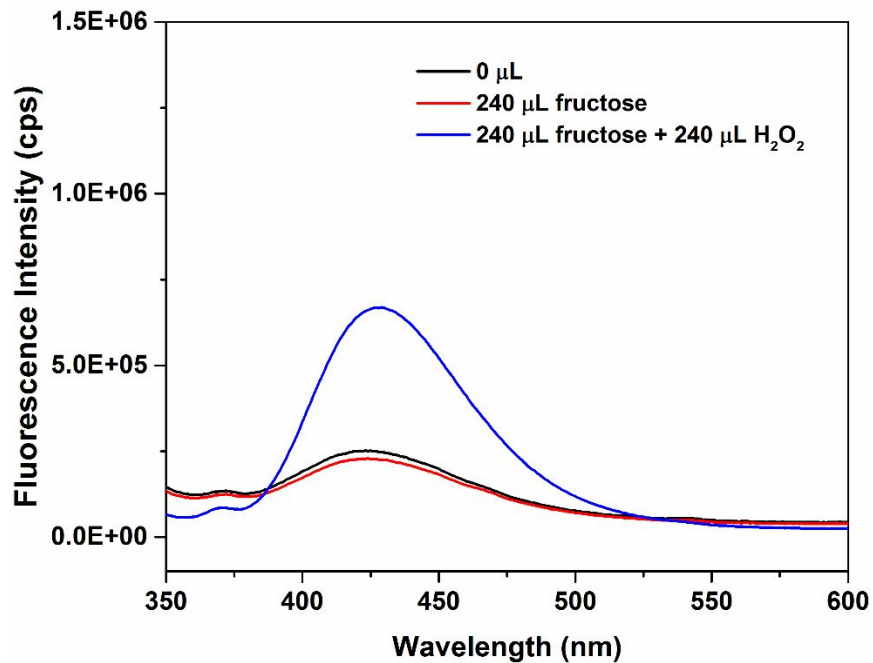


Figure S33. Fluorescence response of **1'** towards 10 mM H_2O_2 in presence of 10 mM fructose ($\lambda_{\text{ex}} = 328$ nm and $\lambda_{\text{em}} = 426$ nm).

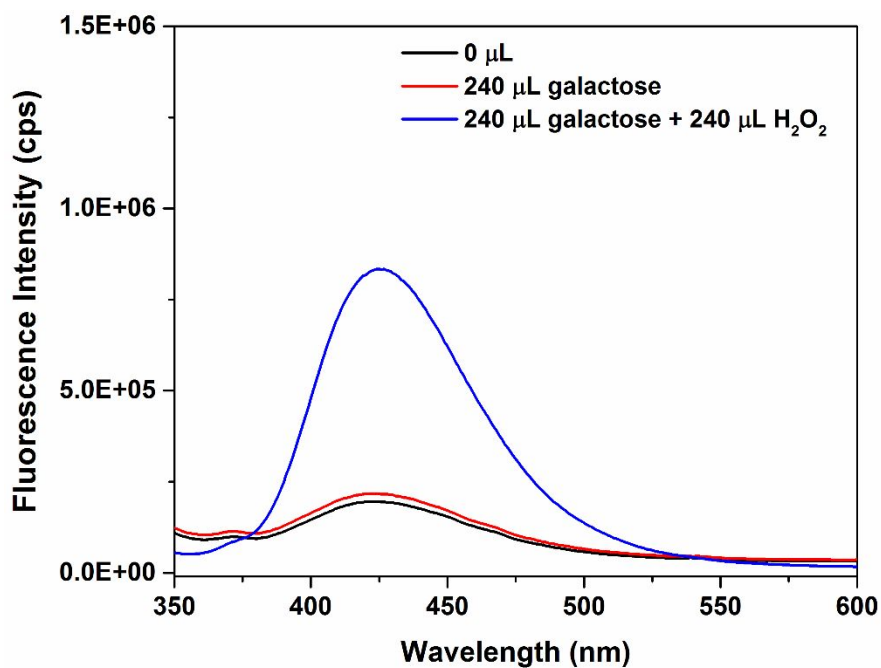


Figure S34. Fluorescence response of **1'** towards 10 mM H₂O₂ in presence of 10 mM galactose ($\lambda_{\text{ex}} = 328$ nm and $\lambda_{\text{em}} = 426$ nm).

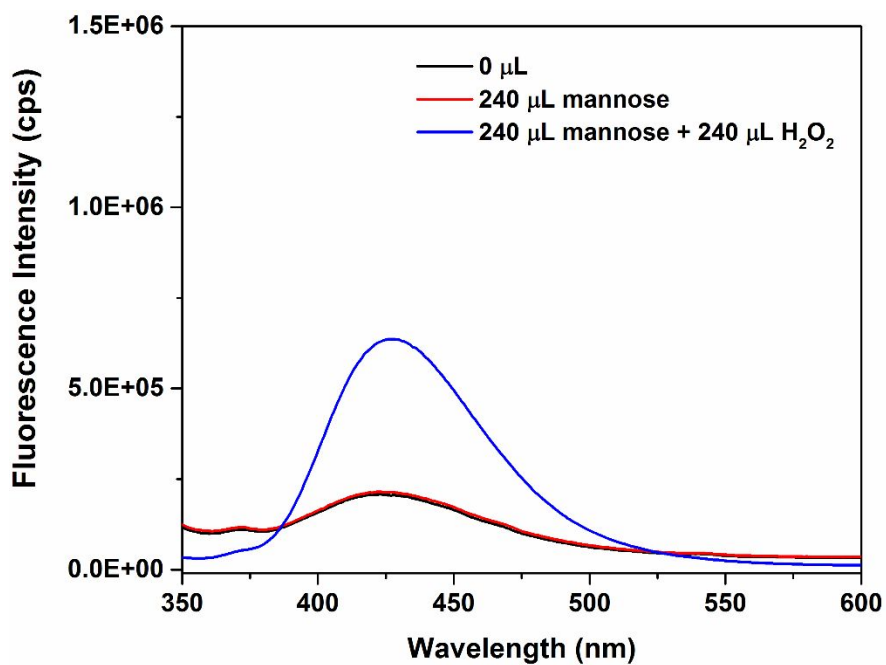


Figure S35. Fluorescence response of **1'** towards 10 mM H₂O₂ in presence of 10 mM mannose ($\lambda_{\text{ex}} = 328$ nm and $\lambda_{\text{em}} = 426$ nm).

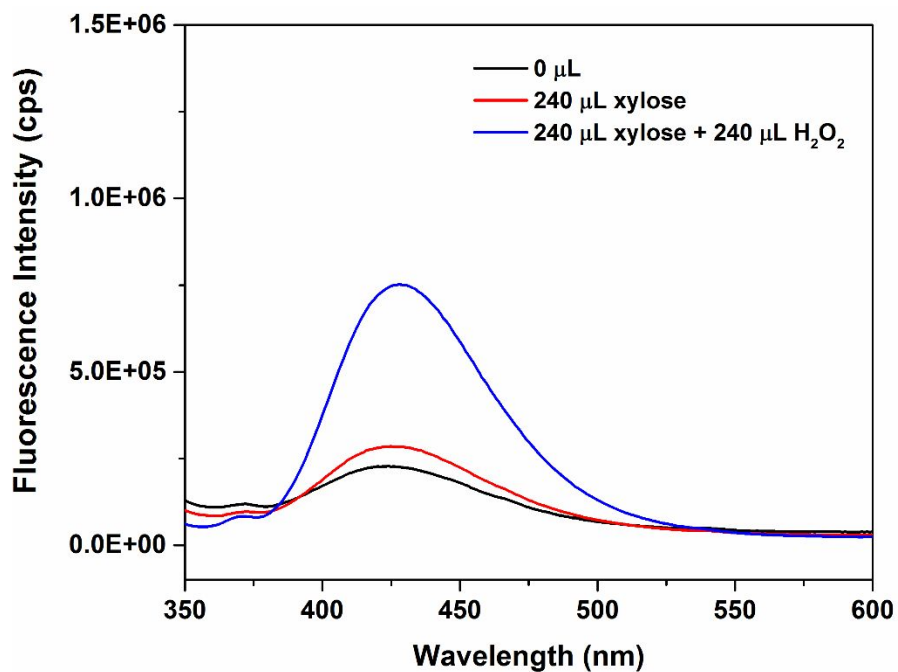


Figure S36. Fluorescence response of **1'** towards 10 mM H_2O_2 in presence of 10 mM xylose ($\lambda_{\text{ex}} = 328$ nm and $\lambda_{\text{em}} = 426$ nm).

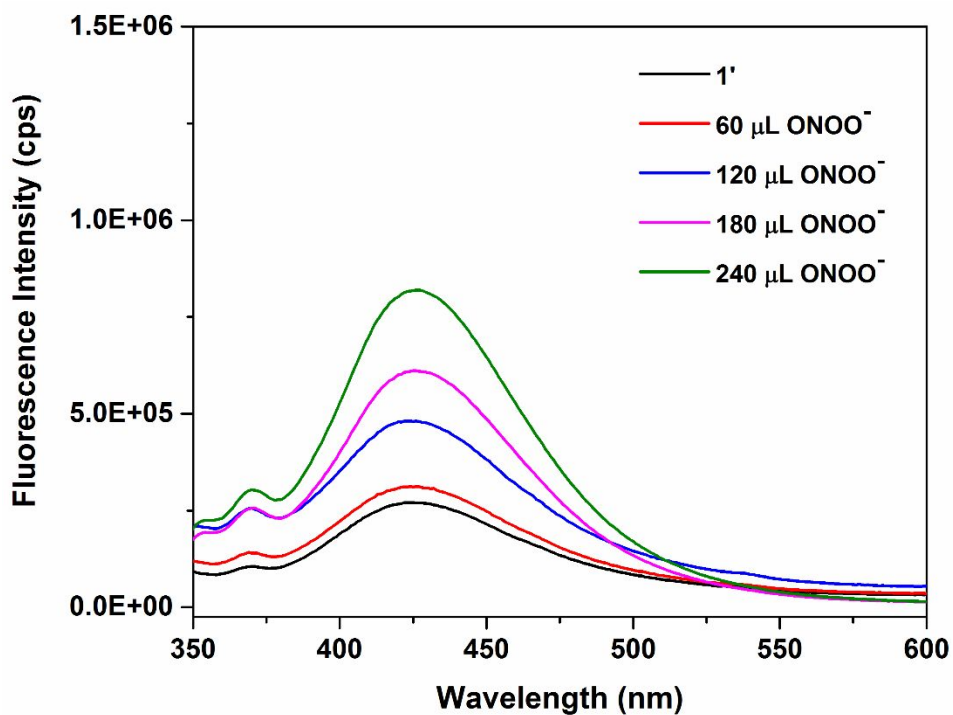


Figure S37. Fluorescence response of **1'** towards 10 mM ONOO^- ($\lambda_{\text{ex}} = 328$ nm and $\lambda_{\text{em}} = 426$ nm).

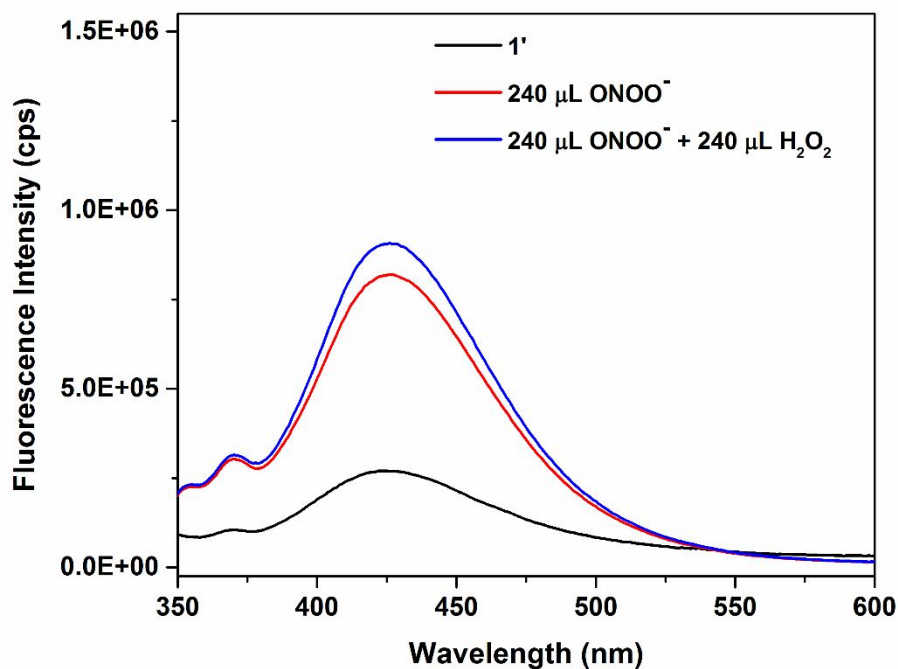


Figure S38. Fluorescence response of **1'** towards 10 mM H₂O₂ in presence of 10 mM ONOO⁻ (λ_{ex} = 328 nm and λ_{em} = 426 nm).

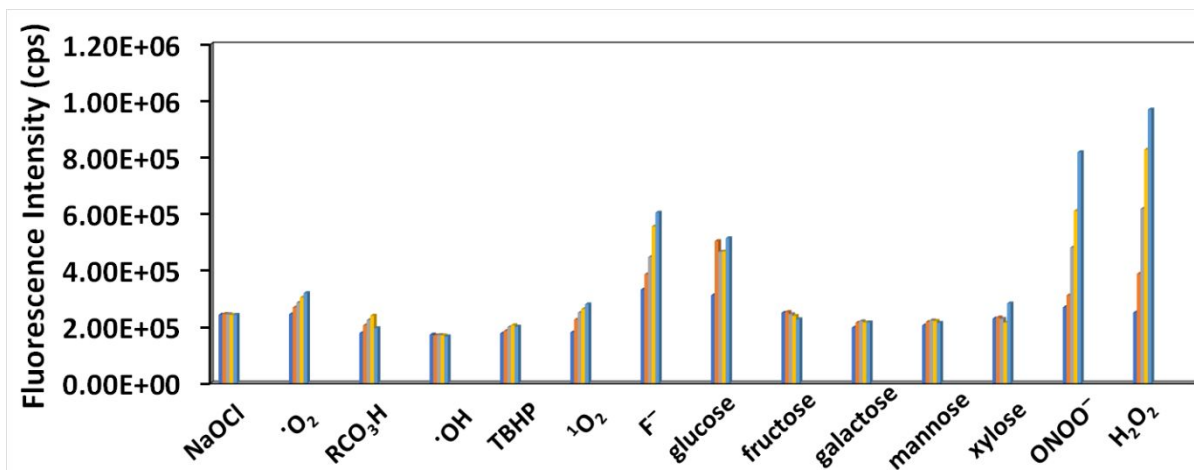


Figure S39. Fluorescence responses of **1'** (suspended in 10 mM HEPES buffer, pH = 7.4) upon the addition of solutions of various ROS (10 mM of ClO⁻, O₂^{•-}, ^tBuO[•], HO[•], TBHP, ¹O₂, ONOO⁻ and H₂O₂) and other biologically relevant species (10 mM of F⁻, glucose, fructose, galactose, xylose and mannose) at room temperature. The bars denote fluorescence intensity after the addition of blank, 60, 120, 180 and 240 μ L of each ROS. The spectra were collected after 6 min of each addition.

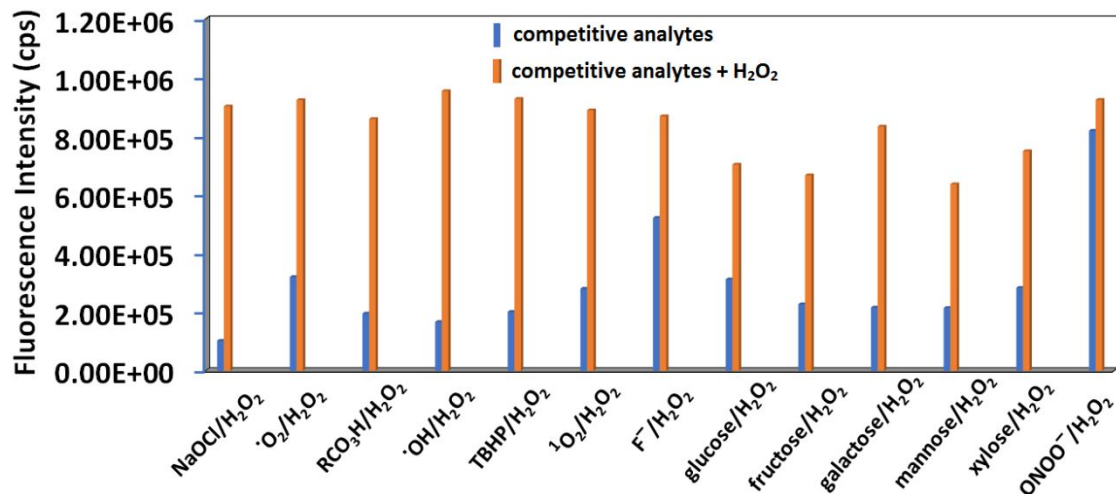


Figure S40. Fluorescence responses of **1'** (suspended in 10 mM HEPES buffer, pH = 7.4) upon the addition of H₂O₂ solution (240 μ L, 10 mM) in the presence of interfering ROS and ONOO⁻ (240 μ L, 10 mM) and other biologically relevant species (240 μ L, 10 mM) at room temperature. The spectra were collected after 30 min of each analyte addition. The final concentration of each analyte in the solution was 9.67×10^{-4} M.

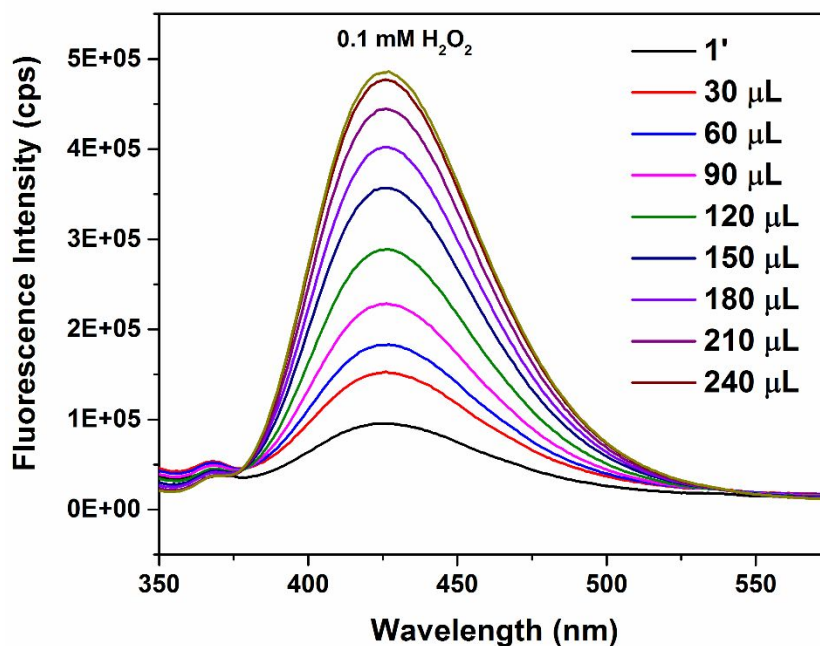


Figure S41. Fluorescence turn-on response of **1'** (suspended in 10 mM HEPES buffer, pH = 7.4) upon the stepwise addition of 0.1 mM H₂O₂ solution at room temperature ($\lambda_{\text{ex}} = 328$ nm and $\lambda_{\text{em}} = 426$ nm).

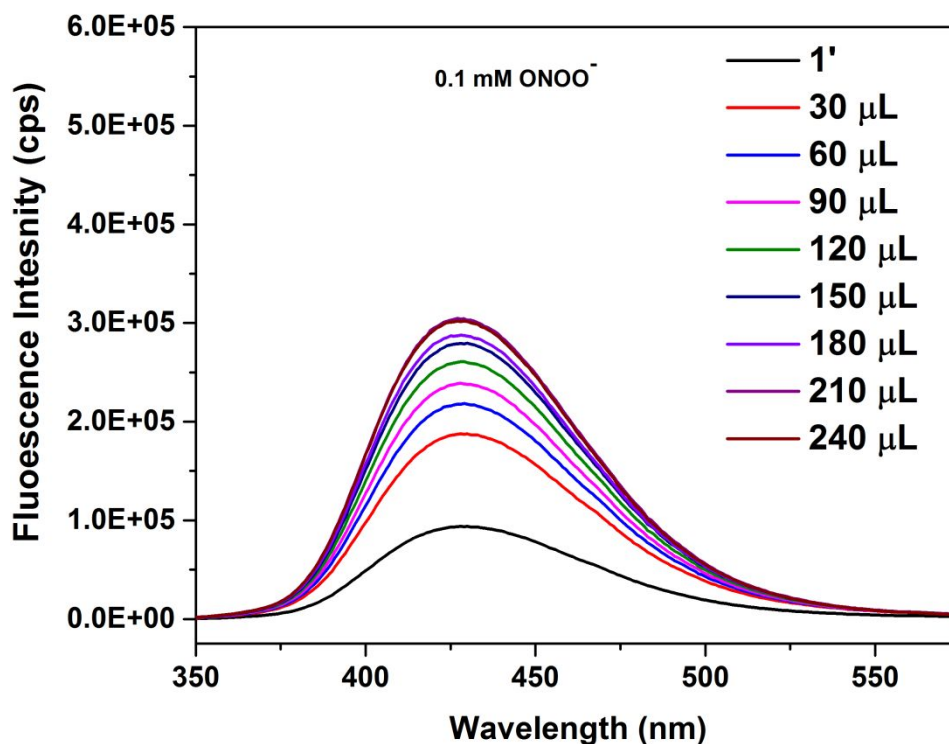


Figure S42. Fluorescence turn-on response of **1'** (suspended in 10 mM HEPES buffer, pH = 7.4) upon the stepwise addition of 0.1 mM ONOO⁻ solution at room temperature ($\lambda_{\text{ex}} = 328$ nm and $\lambda_{\text{em}} = 426$ nm).

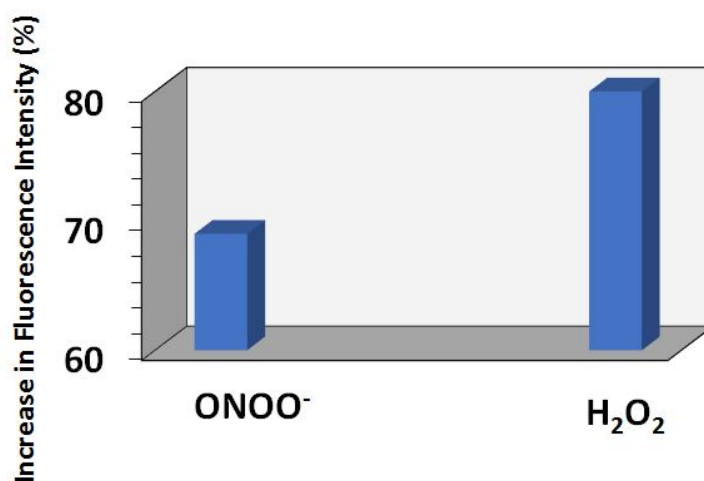


Figure S43. Percentage increases in fluorescence intensity of **1'** (suspended in 10 mM HEPES buffer, pH = 7.4) upon the addition of 240 μL of 0.1 mM of H₂O₂ and ONOO⁻ solutions ($\lambda_{\text{ex}} = 328$ nm and $\lambda_{\text{em}} = 426$ nm).

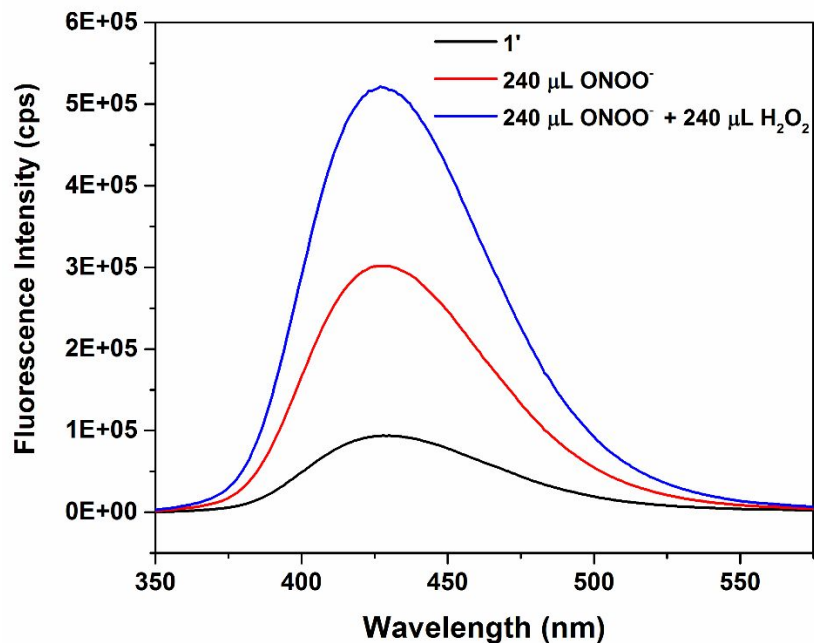


Figure S44. Fluorescence response of **1'** towards 0.1 mM H₂O₂ in presence of 0.1 mM ONOO⁻ ($\lambda_{\text{ex}} = 328$ nm and $\lambda_{\text{em}} = 426$ nm).

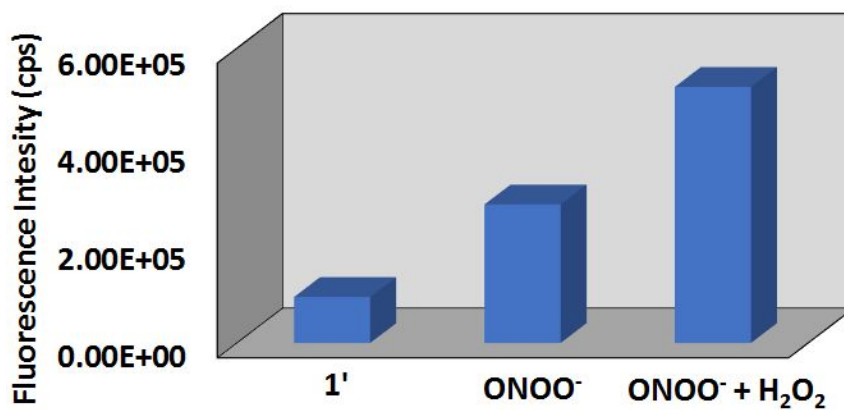


Figure S45. Bar representation showing fluorescence response of **1'** towards 0.1 mM H₂O₂ in presence of 0.1 mM ONOO⁻ ($\lambda_{\text{ex}} = 328$ nm and $\lambda_{\text{em}} = 426$ nm).

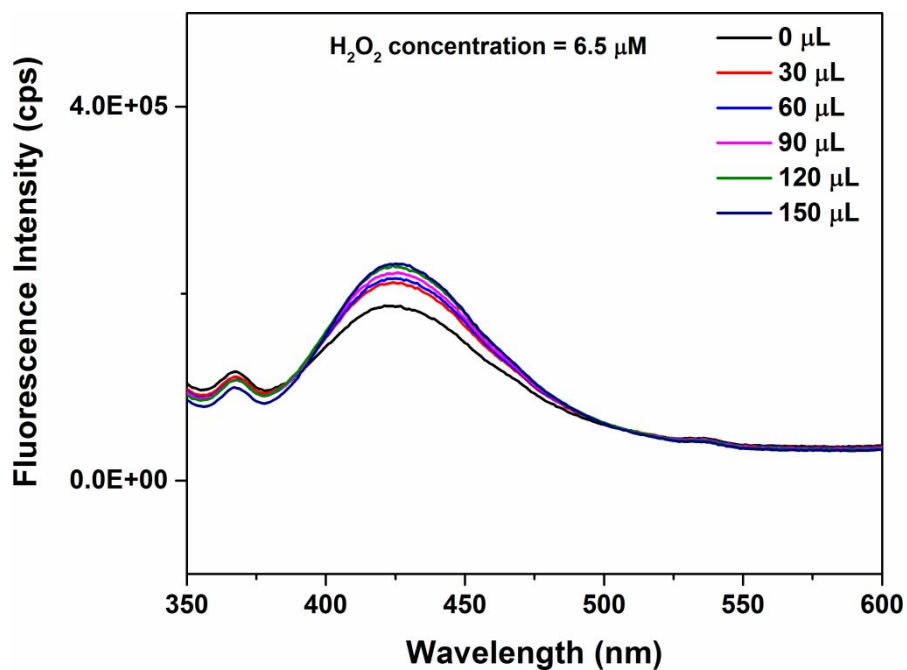


Figure S46. Fluorescence response of **1'** at very low concentration of H₂O₂ ($\lambda_{\text{ex}} = 328 \text{ nm}$ and $\lambda_{\text{em}} = 426 \text{ nm}$).

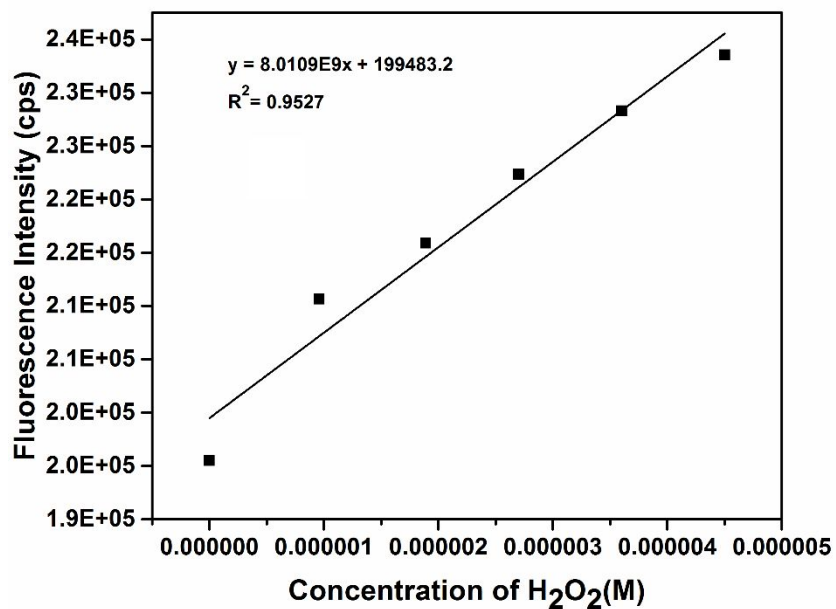


Figure S47. Change in the fluorescence intensity of **1'** in 10 mM HEPES suspension (pH = 7.4) as a function of H₂O₂ concentration.

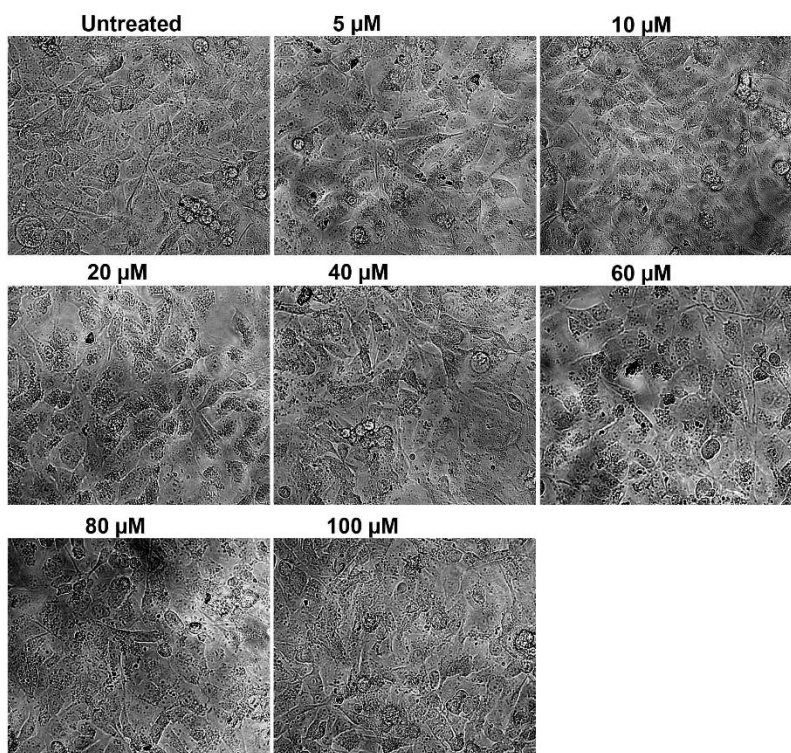


Figure S48. Morphological analysis of untreated cells and the cells treated with various concentrations of **1'**.

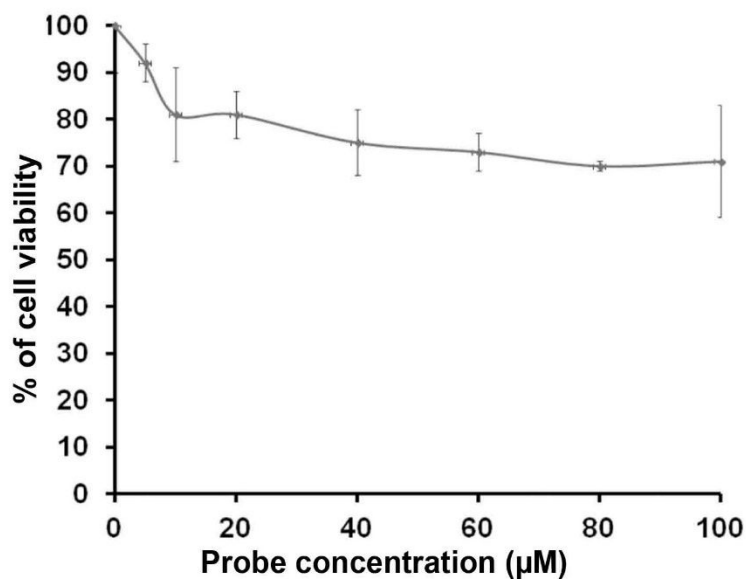


Figure S49. Cell viability assay for **1'**-treated MDAMB-231 cells.

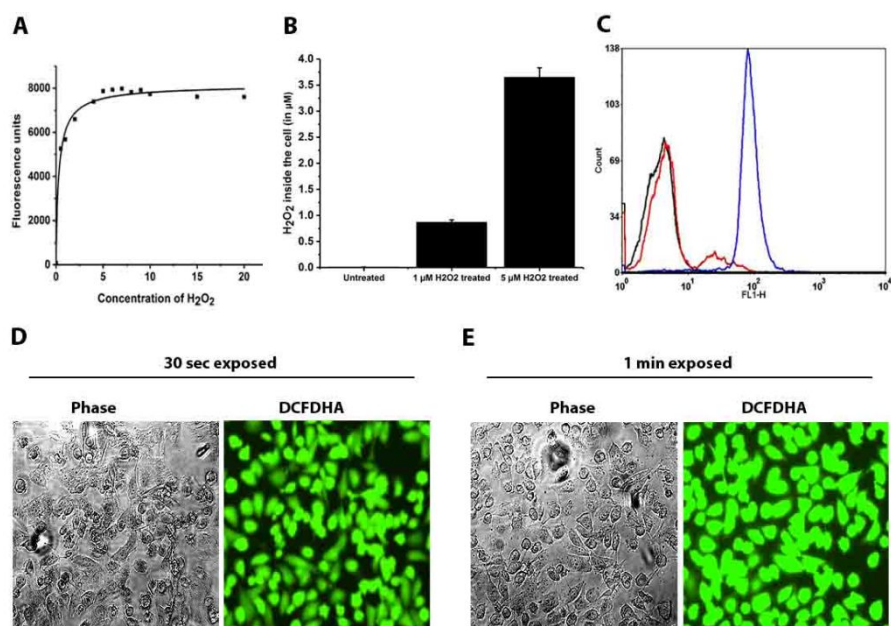


Figure S50. (A) The calibration curve of H₂O₂. The 2'5'-DCFD-HA was incubated with varying concentrations of H₂O₂ and the fluorescence intensity was recorded. (B) Intracellular levels of H₂O₂ as estimated from the cell lysate prepared from MDAMB-231 cells treated with 2'5'-DCFD-HA and exposed to 1 or 5 μM of H₂O₂. (C) The ROS inside the cells was estimated using flow cytometry. As compared with unlabeled cells (black curve), 2'5'-DCFD-HA treated alone (red curve), the 2'5'-DCFD-HA treated cells and exposed to H₂O₂ showed more than 10-fold increase in H₂O₂. (D) and (E) To ascertain the effect of high energy wavelength exposure, the 2'5'-DCFD-HA + H₂O₂ treated cells were exposed to 30 sec and 1 min to monitor any changes in cell morphology.

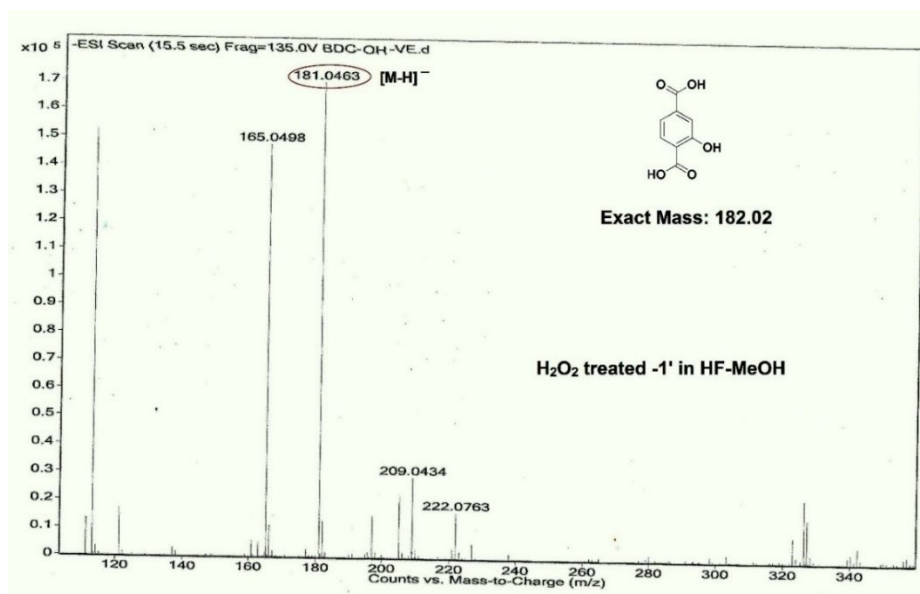


Figure S51. ESI-MS spectrum of H_2O_2 -treated **1'** after digestion in HF/MeOH. The spectrum shows m/z peak at 181.0463, which corresponds to the $[\text{M}-\text{H}]^-$ ion (M = mass of $\text{H}_2\text{BDC}-\text{OH}$ ligand).

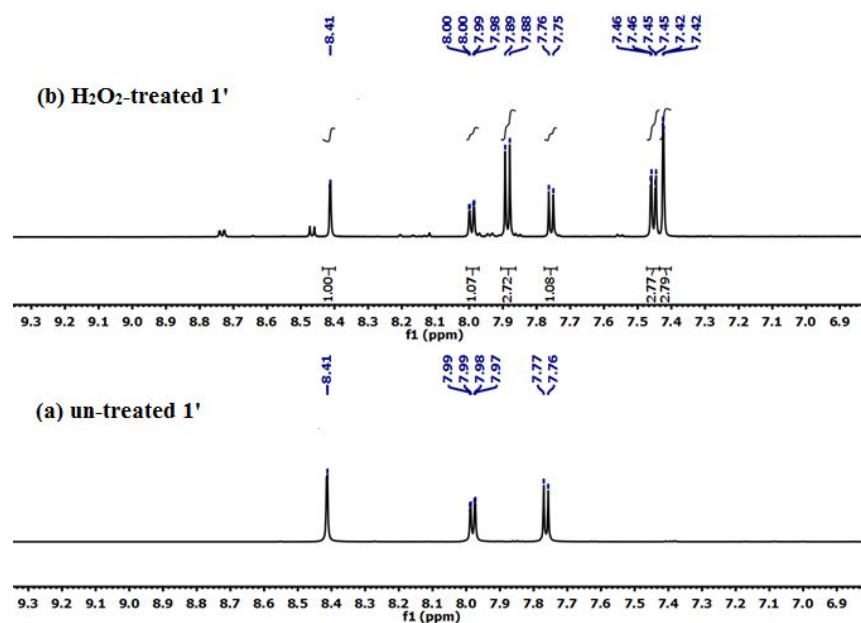


Figure S52. ^1H NMR spectra of (a) un-treated **1'** and (b) H_2O_2 -treated **1'** after digestion in HF/DMSO- d_6 . In the spectrum of H_2O_2 -treated **1'**, new peaks appear at 7.42, 7.45 and 7.88 ppm, which can be assigned to the aromatic protons of the $\text{H}_2\text{BDC}-\text{OH}$ ligand.

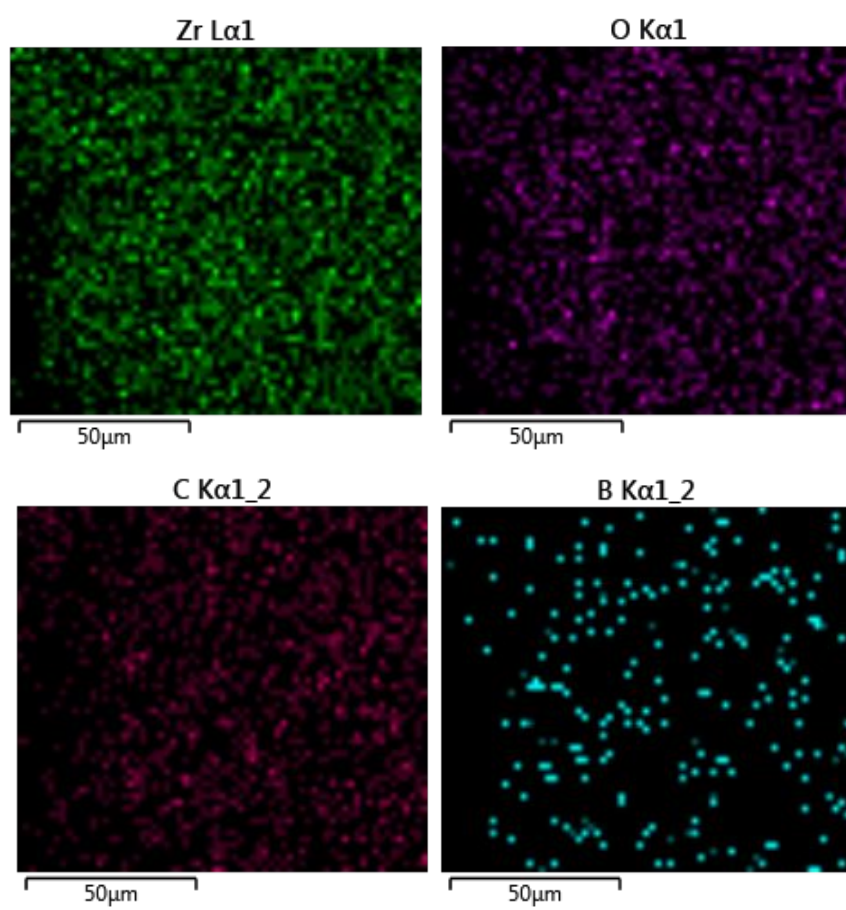
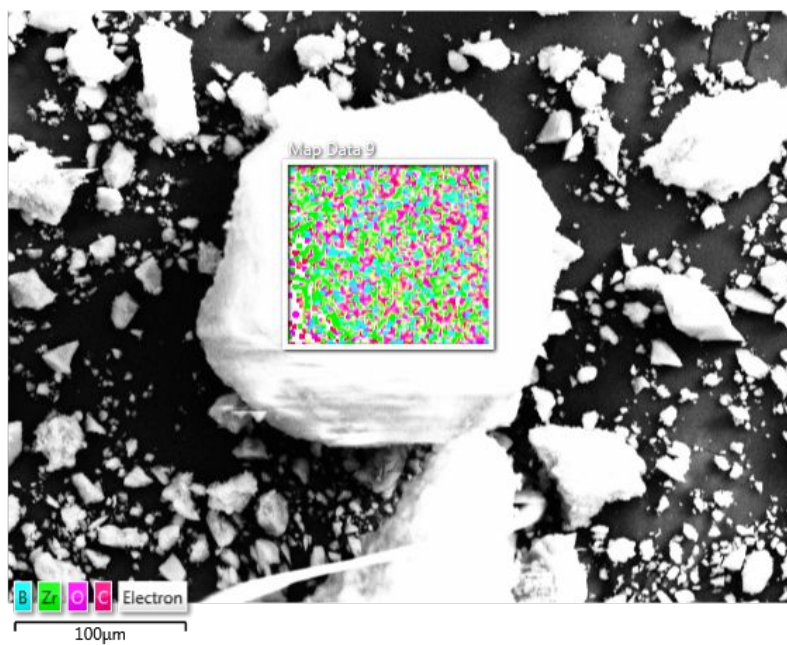
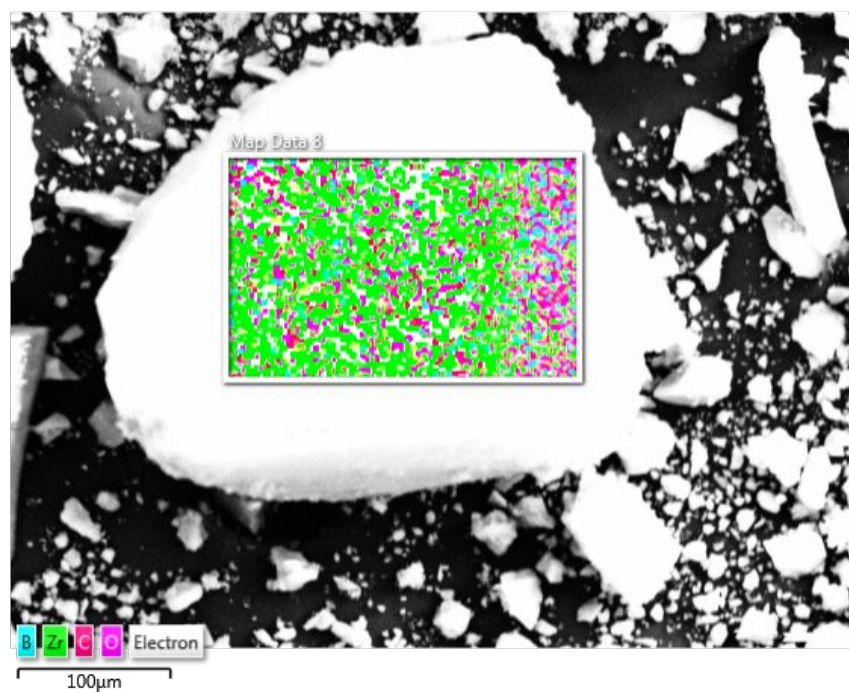
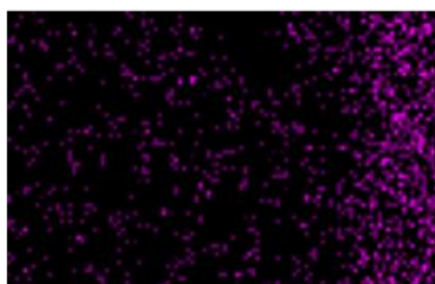
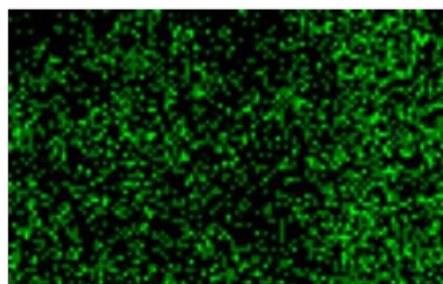


Figure S53. EDX elemental mapping of untreated 1'.



Zr Lα1

O Kα1

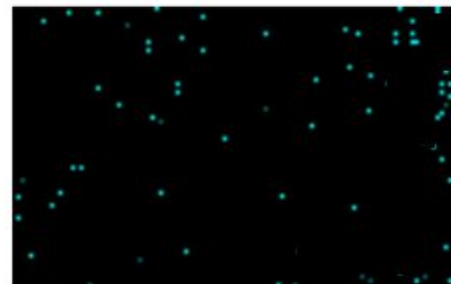
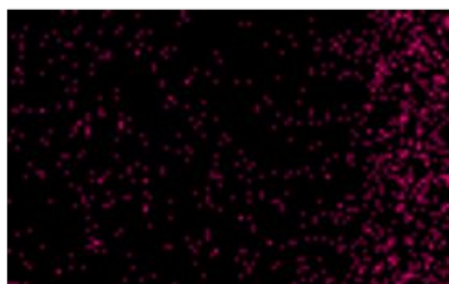


100µm

100µm

C Kα1_2

B Kα1_2



100µm

100µm

Figure S54. EDX elemental mapping of H₂O₂-treated 1'.

Table S1. Comparison of the limit of detection (LOD) values for the H₂O₂ sensing by the MOF materials reported till date using different analytical methods.

Sl. No.	Compound	Limit of Detection (LOD) (μM)	Analytical Method	Reference
1.	hemin@HKUST-1	2.0	chemiluminescence	1
2.	AP-Ni-MOF	0.9	electrochemistry	2
3.	Co/DOBDC	0.5	electrochemistry	3
4.	Cu-MOF	1.0	electrochemistry	4
5.	Co-MOF	3.76	electrochemistry	5
6.	Fe-MIL-53	0.075	electrochemistry	6
7.	Fe-MIL-88	0.562	colorimetry	7
8.	Zr-UiO-66-B(OH) ₂	0.015	fluorescence	This work

Number of Run (n)	Fluorescence intensities (X) at 426 nm before addition of H ₂ O ₂ solution	Mean (\bar{X}_i)	Standard deviation (σ) = $\sqrt{\frac{\sum(X - \bar{X}_i)^2}{n}}$
1.	188116.832	188162.7	40.9
2.	188161.873		
3.	188224.7849		
4.	188120.8757		
5.	188189.0261		

Table S2. Calculation of standard deviation (σ) and LOD#.

$$\#LOD = \frac{3\sigma}{m} = \frac{(3 \times 40.9)}{(8.01 \times 10^9)} = 0.015 \mu\text{M}$$

References:

1. Luo, F.; Lin, Y.; Zheng, L.; Lin, X.; Chi, Y. Encapsulation of Hemin in Metal–Organic Frameworks for Catalyzing the Chemiluminescence Reaction of the H₂O₂–Luminol System and Detecting Glucose in the Neutral Condition. *ACS Appl. Mater. Interfaces* **2015**, *7*, 11322–11329.
2. Sherino, B.; Mohamada, S.; Halima, S. N. H.; Manan, N. S. A. Electrochemical detection of hydrogen peroxide on a new microporous Ni–metal organic framework material-carbon paste electrode. *Sens. Actuators, B* **2018**, *254*, 1148–1156.
3. Zhang, D.; Zhang, J.; Shi, H.; Guo, X.; Guo, Y.; Zhang, R.; Yuan, B. Redox-active microsized metal-organic framework for efficient nonenzymatic H₂O₂ sensing. *Sens. Actuators, B* **2015**, *221*, 224–229.
4. Zhang, D.; Zhang, J.; Zhang, R.; Shi, H.; Guo, Y.; Guo, X.; Li, S.; Yuan, B. 3D porous metal-organic framework as an efficient electrocatalyst for nonenzymatic sensing application. *Talanta* **2015**, *144*, 1176–1181.
5. Yang, L.; Xu, C.; Ye, W.; Liu, W. An electrochemical sensor for H₂O₂ based on a new Co-metal-organic framework modified electrode. *Sens. Actuators, B* **2015**, *215*, 489–496.
6. Cheng, D.; Li, X.; Qiu, Y.; Chen, Q.; Zhou, J.; Yang, Y.; Xie, Z.; Liu, P.; Cai, W.; Zhang, C. A simple modified electrode based on MIL-53(Fe) for the highly sensitive detection of hydrogen peroxide and nitrite. *Anal. Methods* **2017**, *9*, 2082–2088.
7. Gao, C.; Zhu, H.; Chen, J.; Qiu, H. Facile synthesis of enzyme functional metal-organic framework for colorimetric detecting H₂O₂ and ascorbic acid. *Chin. Chim. Lett.* **2017**, *28*, 1006–1012.